Drug Design, Development and Therapy

Dovepress
Taylor & Francis Group

Open Access Full Text Article

ORIGINAL RESEARCH

Zuogui Pill Promotes Neurovascular Regeneration and Corticospinal Tract Remodeling After Ischemic Stroke

Dan Wu[1,*], Xiaohui Yan[1,*], Siqi Mei[1], Hao Hua[1], Xiaoyu Fei[1], Xinyu Xu[1], Yan Liu[1], Minghua Wu[1], Jian Zhu[2], Wenlei Li[1]

[1]Department of Neurology, Jiangsu Province Hospital of Chinese Medicine, Affiliated Hospital of Nanjing University of Chinese Medicine, Nanjing, Jiangsu, People's Republic of China; [2]Department of Endocrinology, Affiliated Hospital of Jiangnan University, Jiangnan University, Wuxi, Jiangsu, People's Republic of China

*These authors contributed equally to this work

Correspondence: Wenlei Li, Department of Neurology, Jiangsu Province Hospital of Chinese Medicine, Affiliated Hospital of Nanjing University of Chinese Medicine, Nanjing, Jiangsu, People's Republic of China, Email yfy120@njucm.edu.cn; Jian Zhu, Department of Endocrinology, Affiliated Hospital of Jiangnan University, Jiangnan University, Wuxi, Jiangsu, People's Republic of China, Email drzhujian@hotmail.com

Video Abstract

Point your SmartPhone at the code above. If you have a QR code reader the video abstract will appear. Or use: https://youtu.be/8lb3MJJkk78

Background: Ischemic stroke (IS) remains a leading cause of long-term disability. Neurovascular regeneration and remodeling of the corticospinal tracts are essential for neurological functional recovery. Zuogui pill (ZGP) has good efficacy in treating cerebral ischemia, but the mechanism remains unclear.

Purpose: To investigate the effects of ZGP on angiogenesis, neurogenesis, corticospinal tract (CST) remodeling, and further evaluate its mechanisms of action in mice with ischemic stroke.

Methods: Network pharmacology was used to analyze the active components, related targets, and mechanisms of ZGP's action in promoting neurovascular regeneration after ischemic stroke. Using a photothrombotic (PT) stroke mouse model, ZGP's effects on neurological recovery were assessed using behavioral tests. Angiogenesis and neurogenesis were evaluated by immunofluorescence of glucose transporter type 1(Glut-1) +/5-bromo-20-deoxyuridine (BrdU) + vessels and doublecortin (DCX)+/BrdU+ cells. CST remodeling was evaluated through diffusion tensor imaging (DTI). The levels of vascular endothelial growth factor (VEGF), brain-derived neurotrophic factor (BDNF), and mammalian target of rapamycin (mTOR) expression were tested by Western blot.

Results: Network pharmacology identified 94 active ingredients and 83 overlapping targets related to IS and neurovascular regeneration. mTOR was identified as one of the core targets. Behavioral tests demonstrated ZGP significantly reduced error rates in irregular ladder walking (ZGP-H vs Stroke: p=0.003) and shortened sticker removal time (ZGP-H vs Stroke: p=0.003). Immunofluorescence revealed ZGP enhanced angiogenesis (Glut-1+/BrdU+ vessels: ZGP-H vs Stroke, p=0.018), neural progenitor cell proliferation and migration (BrdU+/DCX+ cells: ZGP-H vs Stroke: p=0.014). DTI showed increased fractional anisotropy (FA) in ipsilateral CST regions (ZGP-H vs Stroke: $0.001<p<0.05$). Western blot confirmed elevated VEGF (p=0.002), BDNF (p=0.002), and p-mTOR/mTOR ratio ($p<0.001$) in peri-infarct tissues.

Conclusion: ZGP promotes neurovascular regeneration, CST remodeling, and neurological function recovery after ischemic stroke. The positive impacts of ZGP are linked to heightened VEGF and BDNF expression and the activation of the mTOR pathway.

Keywords: zuogui pill, ischemic stroke, angiogenesis, neurogenesis, corticospinal tract remodeling, mTOR

Introduction

Ischemic stroke, accounting for 87% of the 14 million stroke cases worldwide annually according to the World Health Organization (WHO), remains a leading cause of severe neurological dysfunction.[1] Patients who fail to receive vascular recanalization therapy within the critical 4.5–6hour window after symptom onset face high risks of permanent neurological deficits, including hemiparesis, cognitive impairment, speech disorders, and dysphagia. These consequences impose substantial burdens on individuals, families, and society. In developing countries, limited access to timely

Received: 8 February 2025
Accepted: 5 May 2025
Published: 21 May 2025

Graphical Abstract

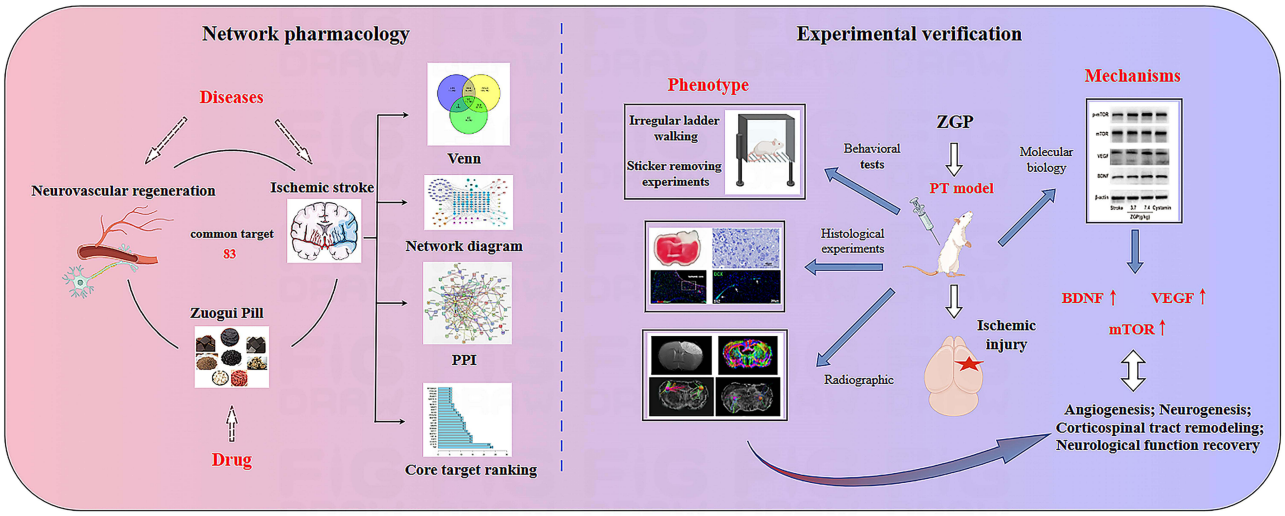

interventions due to restricted therapeutic windows and medical resources often results in lifelong disability for early-onset stroke patients.[2] Following ischemic brain injury, persistent inflammatory responses and degenerative changes hinder the neurovascular system's ability to restore normal function, leading to irreversible deficits.[3]

Neurovascular regeneration and CST remodeling are critical for post-stroke neurological recovery.[4] Mirzahosseini et al[5] demonstrated that vascular endothelial growth factor (VEGF) and brain-derived neurotrophic factor (BDNF) serve as pivotal signaling molecules in these processes. Exogenous administration of VEGF and BDNF has been shown to activate regenerative pathways, mediating angiogenesis, neurogenesis, synaptic remodeling, and functional restoration in experimental stroke models.[6] Central to these mechanisms is the mTOR signaling pathway, which regulates cells' inherent capacity for growth and repair.[7,8] Evidence suggests that crosstalk between BDNF and VEGF activates mTOR signaling, synergistically promoting angiogenesis and neurogenesis.[9] Thus, therapies that elevate BDNF/VEGF levels and stimulate mTOR signaling hold promise for enhancing brain regeneration and neurological recovery after ischemic stroke.

In traditional Chinese medicine (TCM), ischemic stroke pathogenesis is attributed to an imbalance of yin and yang, coupled with kidney essence deficiency, which manifests as cerebral marrow depletion during the recovery phase. Insufficient kidney essence leads to the loss and difficulty in repairing the brain marrow. New blood vessels are created when the kidneys are nourished and the essence is filled, which nourishes the brain marrow and promote its repair.[10] ZGP, a classical TCM formula, is renowned for its ability to tonify kidney yin and generate marrow. Clinical studies have confirmed ZGP's efficacy in improving neurological outcomes in ischemic stroke patients.[11] Preclinical research further supports its neuroprotective properties, promoting axonal regeneration, and anti-inflammatory effects.[12,13] However, whether ZGP promotes angiogenesis, neurogenesis, and CST remodeling—and the underlying mechanisms—remains unclear. In this study, we employed network pharmacology to identify potential targets and pathways of ZGP in treating ischemic stroke. The effects of ZGP on angiogenesis, neurogenesis, CST remodeling, neurological recovery, and the underlying mechanisms were also verified by using a mouse model of ischemic stroke.

Materials and Methods

Prediction and Identification of Active Components and Target Genes of ZGP

Cervi Cornus Colla, Testudinis Carapacis ET Plastri Colla, Rehmanniae Radix Praeparata, Dioscoreae Rhizoma, Corni Fructus, Lycii Fructus, Achyranthis Bidentatae Radix, and Cuscutae Semen are the principal constituents of ZGP. The TCMSP database was used to obtain and validate the primary chemical constituents of the nine medicinal materials that

make up ZGP. Oral bioavailability (OB) ≥ 30% and drug-likeness (DL) ≥ 0.18 are the screening parameters used to find the active ingredients in the Chinese drug composite. Searches were conducted using the HERB and SymMap databases to find medications not listed in the TCMSP database. Targets that were pertinent to drug-related components were found using the SwissTargetPrediction database.

Disease Target Screening

Disease-related targets for ischemic stroke (IS) and neurovascular regeneration were retrieved from the OMIM, GeneCards, and TTD databases using the keywords "ischemic stroke" and "neurovascular regeneration".

Common Targets of ZGP Against Ischemic Stroke and Neurovascular Regeneration

A method of crossing the predicted targets with those of ischemic stroke and neurovascular regeneration was used to identify potential ZGP targets for the treatment of ischemic stroke and the promotion of neurovascular regeneration.

Construction "Herb- Ingredients – Targets" Network Diagram

The drug-disease common targets and potentially active ingredients of ZGP were entered into the Cytoscape3.9.1 program, and the separated components which did not intersect with the targets were eliminated, resulting in the creation of a network diagram of " Herb - Ingredients - Targets diseases".

Protein-Protein Interaction (PPI) Network Analysis

Choose "Homo sapiens" as the protein species and 0.7 as the minimum interaction threshold when searching the above-mentioned STRING database targets. The minimum interaction threshold of 0.7 in the STRING database was selected to ensure high-confidence protein-protein interactions. This threshold balances specificity and biological relevance, avoiding overly dense networks while retaining functionally significant interactions critical for identifying core targets. By removing isolated nodes, PPI network was produced.

Gene Ontology (GO) and Kyoto Encyclopedia of Genes and Genomes (KEGG) Enrichment Analysis

The GO and KEGG enrichment analyses on common targets were carried out using the David database, and the R programming language was utilized to visualize the enrichment outcomes.

Animals and Photothrombotic Focal Stroke Model

The research involved adult male C57BL/6J mice aged 8 to 10 weeks, with weights ranging from 25 to 30 grams and ages between 2.5 and 3 months. The Ethics Committee of the Affiliated Hospital of Nanjing University of Chinese Medicine sanctioned all animal studies (2021 DW-04-02, February 9, 2021). All animal procedures were conducted in accordance with the National Institutes of Health (NIH) Guide for the Care and Use of Laboratory Animals (8th edition, 2011) and the ARRIVE Guidelines 2.0. A photothrombotic stroke model was induced following the method described by Liu et al with minor modifications.[14] Briefly, mice received a tail vein injection of Rose Bengal (10 mg/kg body weight, 5 mg/mL in saline) five minutes before focal illumination of the intact skull. A 4-mm-diameter cold light source (Zeiss CL1500HAL, 150 W, 3000K) was positioned 2.5 mm lateral to Bregma to target the right sensorimotor cortex. Illumination lasted five minutes. Successful induction of the photothrombotic stroke model was confirmed 72 hours post-stroke through two independent validation criteria: MRI T2-weighted imaging demonstrated hyperintense signal by revealing ≥4 distinct ischemic lesions in the right sensorimotor cortex, while the irregular ladder walking test corroborated functional impairment by showing an error rate ≥50% in the injured forelimb compared to pre-stroke baseline performance. These stringent multimodal criteria ensured both structural consistency of ischemic damage and reproducible sensorimotor deficits across experimental cohorts.

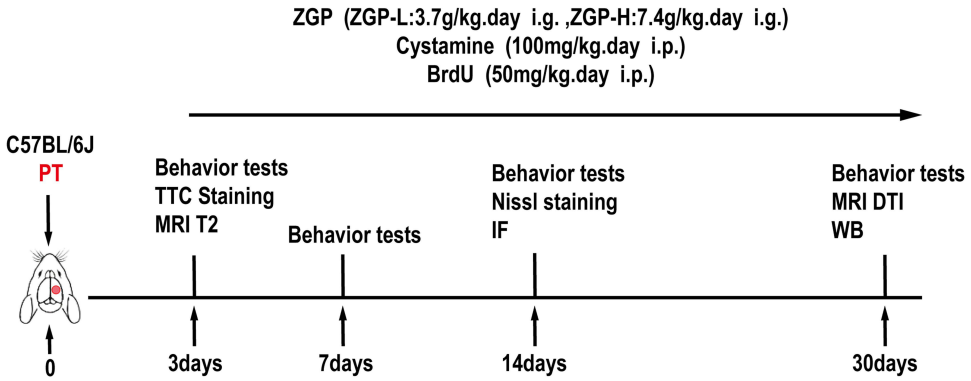

Figure 1 Experimental design timeline for evaluating ZGP's effects in ischemic stroke mice. Mice underwent photothrombotic (PT) stroke induction on Day 0. ZGP (low/high dose), Brdu, and cystamine treatments began on Day 3 and continued until Day 30. Behavioral tests (irregular ladder walking, sticker removing) for evaluating functional recovery were performed pre-stroke (baseline) and post-stroke (Days 3, 7, 14, 30). Histological (Nissl, immunofluorescence) analyses evaluating angiogenesis and neurogenesis were performed at Days 14, and imaging (MRI, DTI) analyses for evaluating CST remodeling were conducted at Days 3 and 30. Western blot analysis for elucidating the mechanisms underlying ZGP's effects was performed at Days 30.

Experimental Design

The outline and flow of the experiment are shown in Figure 1. Cystamine (cystamine dihydrochloride, Sigma, USA) has been shown to enhance axon remodeling, neuronal progenitor cell proliferation, and functional recovery after ischemic stroke.[15] It was selected as a positive control drug in this study. Seventy-two hours post-ischemic stroke induction, the test subjects (40 male C57BL/6J mice in total) were randomized into four groups: Stroke group (Stroke, n=10), low-dose ZGP group (ZGP-L, 3.7 g/kg, n=10), high-dose ZGP group (ZGP-H, 7.4 g/kg, n=10), and Cystamine group (100 mg/kg, intraperitoneally, n=10). The low and high doses of ZGP (3.7 g/kg and 7.4 g/kg, respectively) were selected based on our previous published studies demonstrating efficacy and safety of ZGP in ischemic stroke models.[13] Initially, the human equivalent dose (36.2 g per formulation) was converted to a mouse-equivalent dose using body surface area normalization, multiplied by a safety factor of 3, to establish the highest tested dose (14.8 g/kg for the high-dose group). Subsequent sequential halving generated intermediate and low doses of 7.4 g/kg and 3.7 g/kg, respectively. However, preliminary experiments revealed that 14.8 g/kg induced toxicity and reduced efficacy. Subsequent dose-response evaluations confirmed that 7.4 g/kg and 3.7 g/kg achieved optimal therapeutic effects without adverse effects, justifying their selection for this study. The ZGP solution was prepared in saline and administered via oral gavage once daily. The stroke group received an equivalent volume of saline alone using the same regimen. Cystamine was dissolved in 0.09% saline and given intraperitoneally every day. To identify proliferating cells, each animal was administered intraperitoneal injections of BrdU (Sigma, USA) dissolved in 1×PBS buffer at a daily dose of 50 mg/kg. All interventions started on day 3 and continued to day 30 days after ischemia induction. Behavioral tests were performed pre-stroke and on days 3, 7, 14, and 30 post-stroke to assess motor and sensory functions of mice. On day 14 of ischemia induction, Nissl and immunofluorescence staining were used to observe histopathological changes, angiogenesis, proliferation and migration of neural progenitor cells. On day 30 of ischemia induction, 7.0T MRI diffusion tensor imaging (DTI) was performed to visualize the remodeling of CST in mice, and BDNF, VEGF, and mTOR protein expression in peri-infarct tissues was examined by protein immunoblotting.

ZGP Preparation

A single dose of ZGP consists of a blend of 8 traditional Chinese herbs in the proportions of 8: 4: 4: 4: 3: 4: 4: 4, which includes 24g of *Rehmanniae Radix Praeparata*, 12g of *Dioscoreae Rhizoma*, 12g of *Corni Fructus*, 12g of *Lycii Fructus*, 9g of *Achyranthis Bidentatae Radix*, 12g of *Cervi Cornus Colla*, 12g of *Testudinis Carapacis ET Plastri Colla*, and 12g of *Cuscutae Semen*. All the herbs originated in China. The ZGP, created by the pharmacy department at Jiangsu Provincial Hospital of Chinese Medicine, was validated using the 2015 edition of the Chinese Pharmacopoeia. The pharmacy at Jiangsu Provincial Hospital of Chinese Medicine obtained a reference sample (2023–0615). ZGP was prepared according to the method described in the previous study.[13,16,17] 30 prescriptions (3150g) were made in total, and

1086g of ZGP-dried powder were produced. The substance was stored in portions at −20°C. ZGP has been analyzed by UPLC-QTOF-MS assay, and detailed information can be obtained by referring to our previously published article.[16]

Irregular Ladder Walking Test

The capacity for ladder walking was evaluated in various mouse groups employing a method detailed in earlier studies.[13,14] Proper movements (Hit) occur when the palm's center is accurately positioned on the rung for both front and back limbs, with the fingers of the front limbs closed. The leftover instances were classified as errors, divided into two types: 1) Miss: When a mouse is moving along the ladder, its forelimb or hindlimb either completely misses the rung or touches it with the wrist or heel instead of the paw; 2) Slip: When a mouse uses only a few fingers instead of the paw to grip the rungs, leading to a subsequent slide. The results were presented using the (Miss + Slip) / (Hit + Miss + Slip).

Sticker Removing Test

Prepare stickers with a size of 3mm × 3mm, apply them to the center of the mouse's forelimb palm with ophthalmic forceps, and place the mouse in a transparent glass device. Record the time it takes for the mouse to perceive and remove the sticker, with a maximum recording time of 2 minutes. All experimental animals were tested on one side of the forelimb palm and then the other side. Each mouse was tested 3 times before the induction of ischemia, and the average of the 3 tests was used as the baseline.

Triphenyl Tetrazolium Chloride (TTC) Staining

On the third day after focal cerebral ischemia, the brains of mice were cut into 1mm thick coronal slices from front to back in a mouse brain mold. Brain sections were immersed in PBS solution with 1% TTC and kept at 37°C for 15 minutes. The brain sections, which were stained, were submerged in a 4% paraformaldehyde (PFA) phosphate buffer solution and left to be fixed for a day.

Immunofluorescence Staining

Two weeks post-stroke, brains preserved in paraffin were cut into 4μm thick coronal sections, and immunohistochemistry was conducted following the methods outlined by Li et al.[18,19] The primary antibodies employed for single or double staining included rat anti-BrdU (1:400; Abcam) for cell proliferation, goat anti-doublecortin (DCX; 1:200; Santa Cruz Biotechnology) for migrating neuroblasts, and rabbit anti-Glut-1 (1:1000; Chemicon, Temecula, CA) for endothelial cells. Secondary antibodies used were Alexa Fluor 488 anti-rat, anti-goat, anti-rabbit IgG (1:200; Invitrogen, Carlsbad, CA), or Cy3-conjugated anti-rat IgG (1:1000; Invitrogen). The staining was observed using fluorescent and confocal microscopy (BX61; Olympus, Tokyo, Japan). For each mouse, three coronal brain sections were selected for cell counting, with each slice separated by 300μm within the same target area. In the ischemic border area, four fields per brain slice were randomly selected for multistage random sampling. Every counting assay was carried out under blind conditions.

Nissl Staining

After paraffin-embedded brain slices were deparaffinized, the slices were immersed in cresyl violet for 2–3 minutes. The excess staining solution was rinsed off with water, and the sections were differentiated with glacial acetic acid and observed under the microscope. Differentiation was continued until the background turned light blue and the nidus turned dark blue. The differentiation process was stopped and the neuronal cells morphology was observed under the microscope in randomly selected fields around the infarct area.

Western Blot Analysis

According to our earlier study,[18] the peri-infarct region was defined by a 500μm boundary stretching from the medial, lateral, and infarct edges toward the infarct. Proteins were isolated from tissue specimens of the peri-infarct region through homogenization in a protein lysis solution. The amount of protein was measured through the BCA method. The SDS-PAGE gel electrophoresis was performed at 80 volts for half an hour, followed by 120 volts for one hour. To convert the membrane, a steady current was applied of 250 mA for 90 minutes, then cool it on ice, and finally, seal it with

skimmed-milk powder for an hour at 25°C. The membranes were stored at 4°C overnight with one of these primary antibodies: mouse anti-mTOR (1:5000), rabbit anti-p-mTOR, rabbit anti-VEGF, mouse anti-BDNF, or mouse anti-β-actin. Following a one-hour incubation with secondary antibodies (goat anti-rabbit IgG at 1:5000 or goat anti-mouse IgG at 1:2000) and a 30-second to two-minute exposure to ECL reagents, the membranes were placed on Kodak film (Japan). Use ImageJ program to measure and evaluate IOD ratios to display the data.

Magnetic Resonance Imaging (MRI)

Thirty days post-stroke, MRI scans were conducted on mice utilizing a 7.0 Tesla small animal MRI system (Bruker PharmaScan, Ettlingen, Germany) as described in a prior study.[15] The ImageJ software (National Institutes of Health, Bethesda, MD, USA) was utilized to determine the infarct volume by subtracting the volume of the uninjured ipsilateral hemisphere from that of the contralateral hemisphere in T2-weighted images. Subsequently, a computerized analysis was performed to express the infarct volume as a percentage, calculated by dividing the infarct volume by the volume of the contralateral hemisphere. Diffusion tensor imaging (DTI) revealed injury to the corticospinal tract within the sensorimotor cortex and internal capsule. An echo-planar imaging (EPI) sequence was parameterized with 30 distinct diffusion directions and 5 reference images. Paravision 5.0 software (Bruker Biospin, Ettlingen, Germany) was employed to compute fractional anisotropy (FA), focusing on the anatomical regions of the corpus callosum and hippocampus for localization. Areas of interest (ROIs) were outlined on FA maps within the sensory-motor cortex and corpus callosum across five brain image planes called Genu, Body, Dorsal fornix, Dorsal syndesis, and Dentate gyrus. Fiber bundle tracts were reconstructed, visualized, and examined with Diffusion Toolkit (v0.6.2.1) and TrackVis (v0.5.2.1) software. Regions of interest (ROIs) were chosen for the motor-sensory cortex at the corpus callosum's knee and for the internal capsule structures at the hippocampus dentate gyrus level.

Statistics

The data are presented as the average value plus or minus the standard error of the mean. Each experiment was performed as a separate, independent experiment. To minimize bias, all behavioral assessments, histological analyses, and data quantification were conducted by investigators blinded to experimental group assignments. Group labels (eg, Stroke, ZGP-L, ZGP-H, Cystamine) were anonymized during data collection and analysis. Quantitative and statistical analyses of imaging, molecular biology, histological regional results, and immunofluorescence staining cell count results were performed using ImageJ software. The software GraphPad Prism 9, based in La Jolla, California, USA, was utilized for creating plots. To evaluate group differences, we employed one-way Analysis of Variance (ANOVA), the Brown-Forsythe test, multiple-comparison methods, and Tukey's multiple comparisons test. A P-value below 0.05 suggests a meaningful statistical outcome.

Results

Construction of "Herb- Ingredients – Targets" Network Diagram

After filtering and removing duplicates, 94 potentially active ingredients were identified from ZGP, including 4 from *Achyranthis Bidentatae Radix*, 45 from *Lycii Fructus*, 6 from *Testudinis Carapacis ET Plastri Colla*, 5 from *Cervi Cornus Colla*, 16 from *Dioscoreae Rhizoma*, 20 from *Corni Fructus*, 2 from *Rehmanniae Radix Praeparata*, 11 from *Cuscutae Semen*. Using the SwissTargetPrediction database, 711 potential drug targets associated with these ingredients were screened. Concurrently, disease-related targets for ischemic stroke (IS) and neurovascular regeneration were retrieved from the OMIM, GeneCards, and TTD databases, yielding 7,424 unique ischemic stroke targets and 444 neurovascular regeneration targets after deduplication. A Venn diagram intersecting ZGP targets (711), ischemic stroke targets (7,424), and neurovascular regeneration targets (444) revealed 83 common targets (Figure 2A). These overlapping targets were further visualized in a "Herb-Ingredients-Targets" network to integrate active ingredients, their herbal sources, and shared disease-related mechanisms (Figure 2B). This network highlights ZGP's multi-component, multi-target therapeutic profile, with node sizes reflecting interaction degrees to prioritize core targets for subsequent analysis.

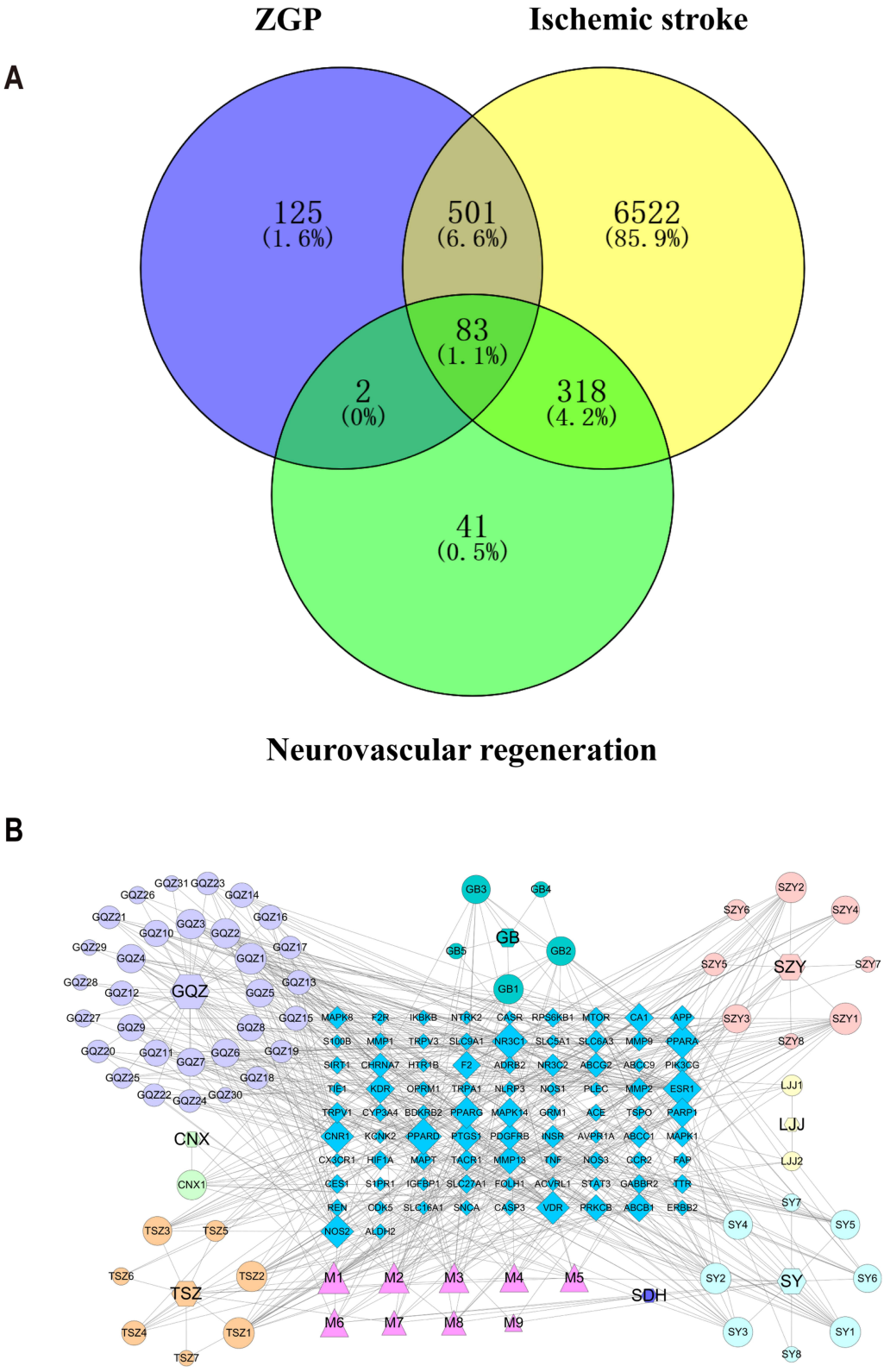

Figure 2 Network pharmacology analysis of ZGP's active components and targets. (**A**) Venn diagram illustrating the intersection of ZGP-related targets (711), ischemic stroke-related targets (7,424), and neurovascular regeneration-related targets (444), identifying 83 common therapeutic targets. (**B**) The network diagram of "Herb-Ingredients-Targets". The hexagons in the graph represent the drugs, the circles represent the respective unique components of each drug, the triangles represent the common components of the drugs, the diamonds represent the 83 common targets, and the node sizes vary depending on the size of the node degree value. There are 162 nodes and 574 edges in the graph. The network highlights ZGP's multi-component, multi-target therapeutic profile, with core targets prioritized for mechanistic investigation.

https://doi.org/10.2147/DDDT.S518696

PPI Network Construction and Core Target Analysis

The 83 drug-disease common targets were imported into the STRING database to create a PPI network of protein interactions (Figure 3A). To map the network of protein interactions, the resulting network data was imported into the

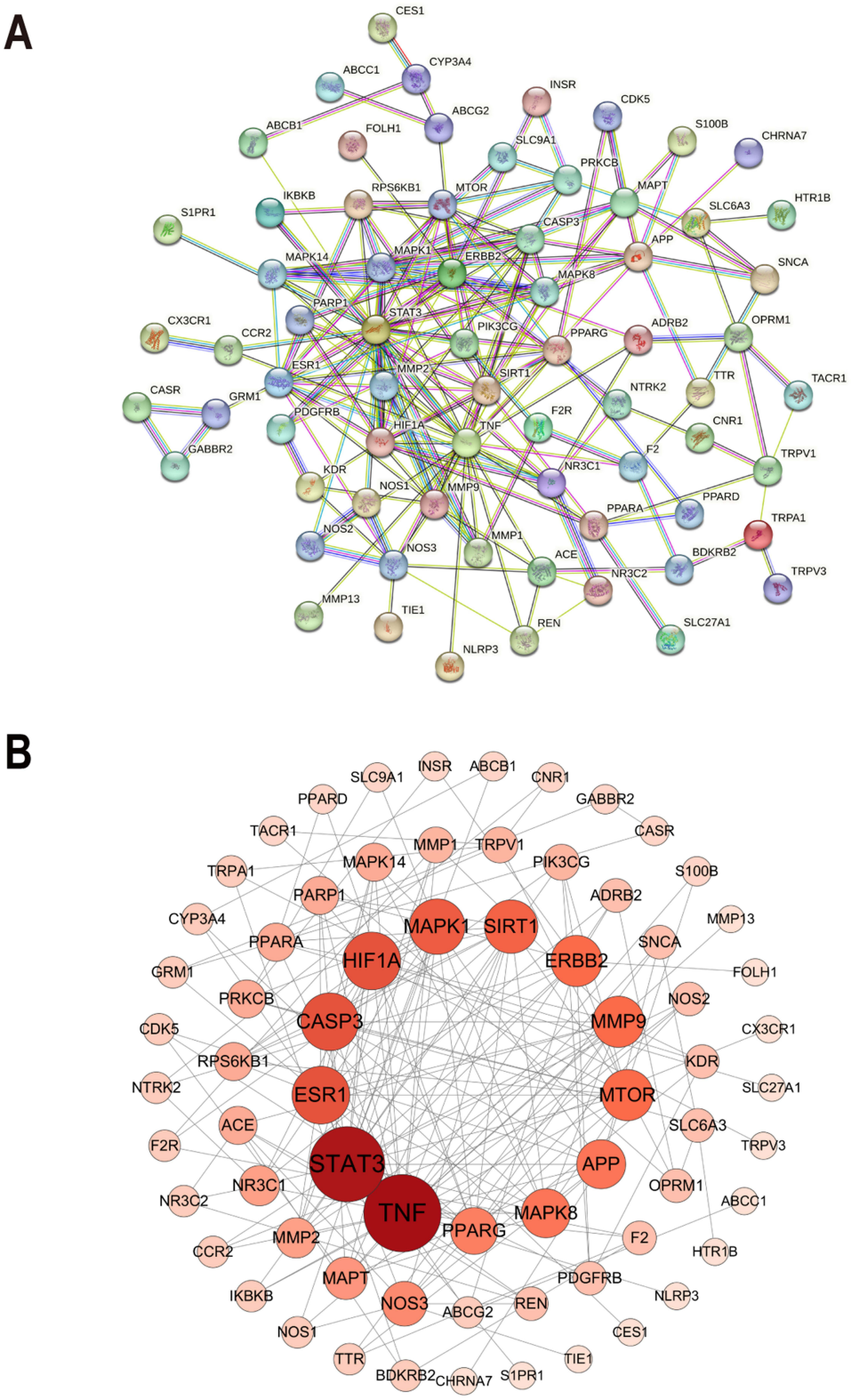

Figure 3 Continued.

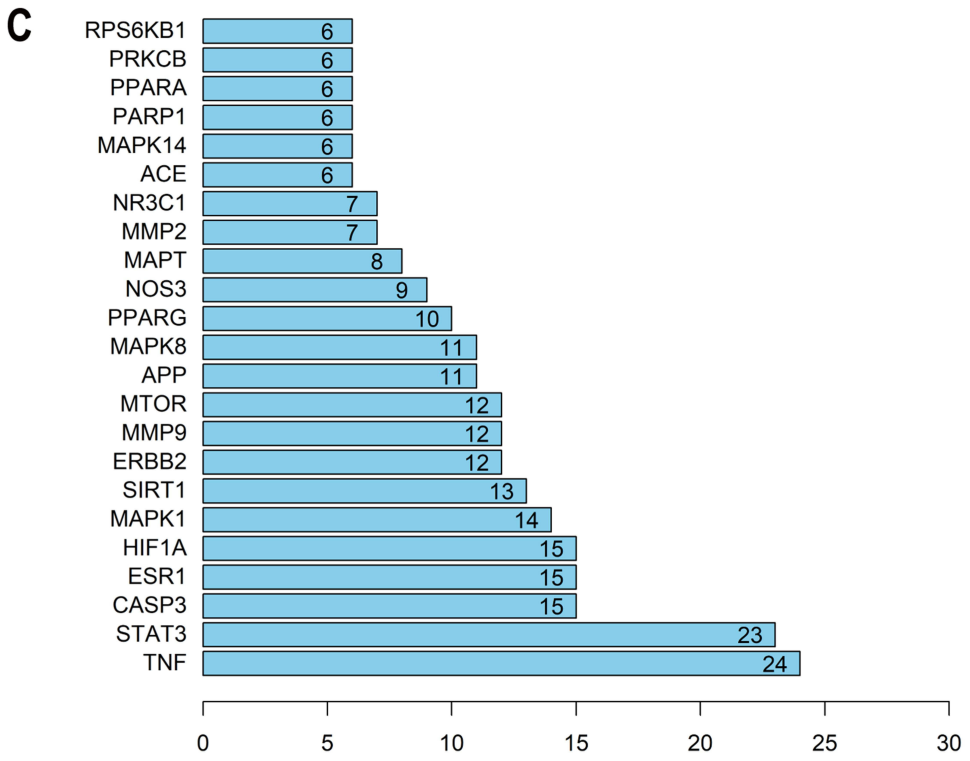

Figure 3 PPI network construction and core target analysis. (**A**): PPI network of 83 common targets related to ZGP, ischemic stroke, and neurovascular regeneration, generated using the STRING database. Node sizes (69 nodes and 187 edges) and color intensity reflect degree values (larger/darker nodes = higher connectivity). (**B**): Refined network visualized in Cytoscape, highlighting densely connected modules. (**C**): Top 20 core targets ranked by degree centrality. Key targets such as TNF, STAT3, mTOR, and MMP9 exhibit high degrees, indicating their pivotal roles in neurovascular regeneration and ischemic stroke recovery.

Cytoscape program to import the PPI network (Figure 3B). NetworkAnalyzer tool was used to perform a topology analysis and find core targets according to degree values. The top 20 targets ranked by degree values were subsequently plotted as a bar graph using R 4.2.1 (Figure 3C), highlighting key nodes such as tumor necrosis factor (TNF), signal transducers and activators of transcription 3 (STAT3), mTOR, and matrix metalloproteinase 9 (MMP9), which exhibited the highest connectivity and are critically implicated in neurovascular regeneration pathways.

Analysis of GO and KEGG Enrichment

According to the results of GO enrichment analyses, a total of 387 biological processes (BPs), 52 cellular components (CCs), and 93 molecular functions (MFs) were enriched for overlapping genes. The top 10 significantly enriched terms (ranked by P-value) for each category were visualized as bar and bubble charts (Figure 4A and B). For biological processes (BPs), the most enriched terms included response to xenobiotic stimulus, positive regulation of phosphatidylinositol 3-kinase/protein kinase B signaling, and transport across the blood-brain barrier. Key cellular components (CCs) comprised the plasma membrane, receptor complexes, and membrane rafts, while predominant molecular functions (MFs) involved identical protein binding, nuclear receptor activity, and peptidase activity. KEGG pathway analysis using the DAVID database identified 115 enriched pathways. The top 20 pathways with the lowest P-values were visualized in bar and bubble charts (Figure 5A and B), where warmer colors (eg, red) indicated higher significance (-log10[P-value]). Major signaling pathways included proteoglycans in cancer, pathways in cancer, insulin resistance, calcium signaling, HIF-1 signaling, neuroactive ligand-receptor interaction, diabetic cardiomyopathy, IL-17 signaling, and relaxin signaling.

ZGP's Influence on Infarct Size in Mice After Ischemic Stroke

A reproducible cortical infarction was established using the method of photochemical thrombosis, which unilaterally destroys the sensory motor cortex (Figure 6A and B). On day 3 after cerebral ischemia, TTC staining showed complete

https://doi.org/10.2147/DDDT.S518696

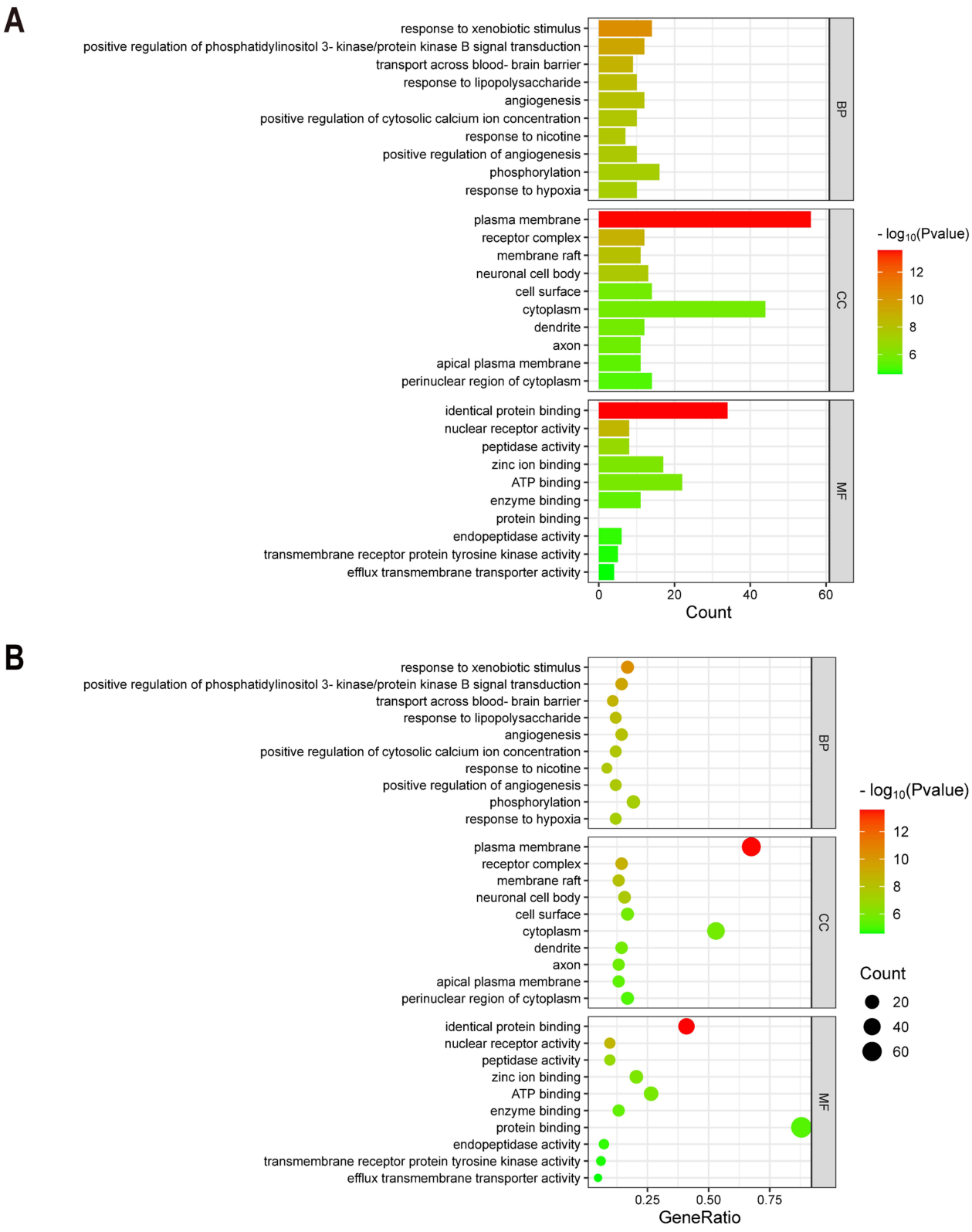

Figure 4 GO enrichment analysis of ZGP targets. (**A**): Bubble chart displaying the top 10 enriched GO terms (Biological Process, BP; Cellular Component, CC; Molecular Function, MF). Bubble size represents gene count; color intensity reflects −log10(*p*-value). Key processes include "response to xenobiotic stimulus" (BP), "plasma membrane" (CC), and "identical protein binding" (MF). (**B**): Bar graph summarizing the top 10 enriched GO terms across all categories, ranked by statistical significance. Together, these results highlight ZGP's multi-faceted roles in neurovascular regeneration, spanning cellular localization, molecular interactions, and signaling pathway modulation.

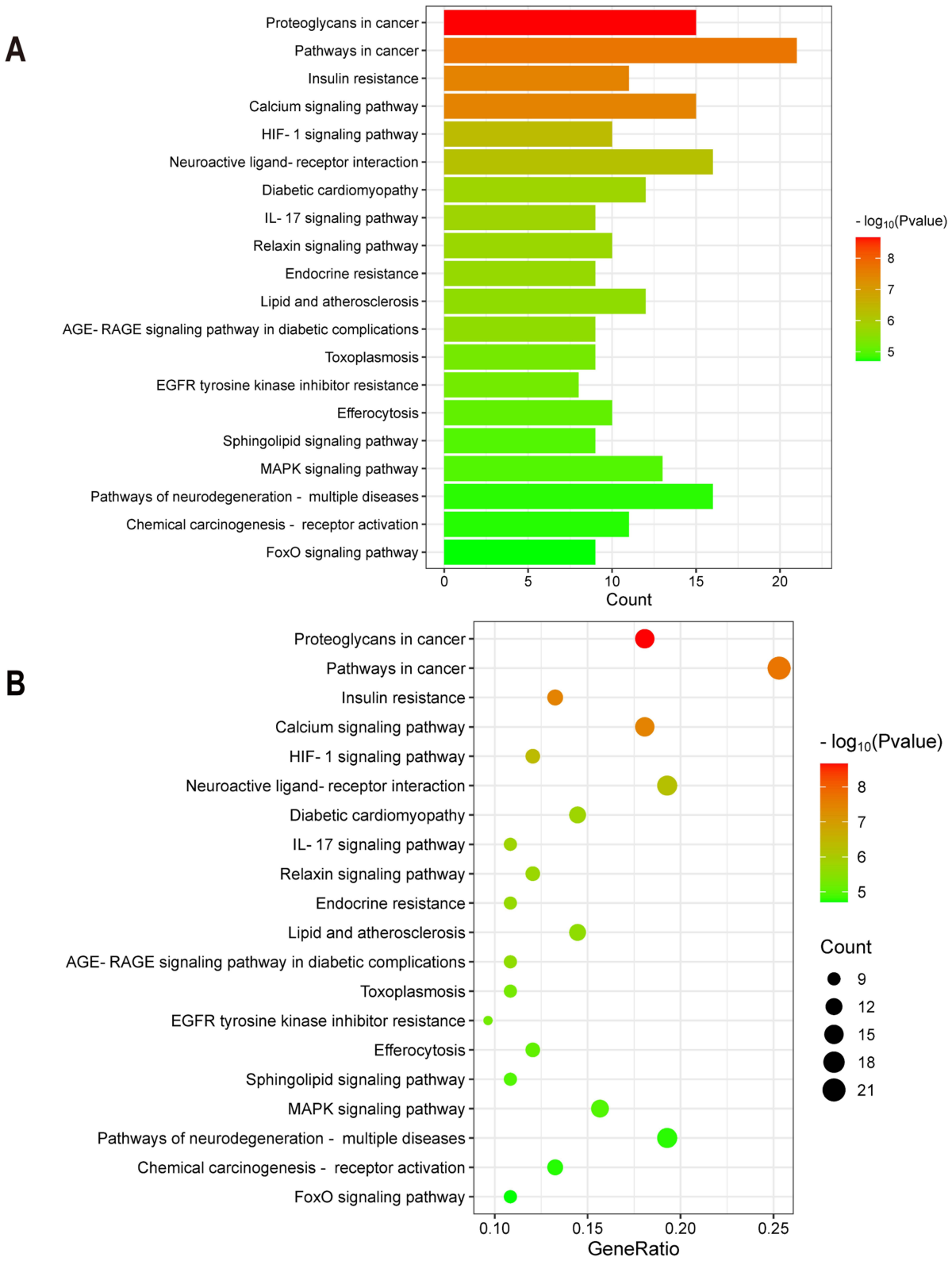

Figure 5 KEGG pathway enrichment analysis of ZGP targets. **(A)**: Bubble chart of the top 20 enriched KEGG pathways ranked by statistical significance. Bubble size represents the number of genes associated with each pathway, and color intensity reflects the −log10(P-value) (redder hues indicate higher significance). Key pathways include HIF-1 signaling, neuroactive ligand-receptor interaction, calcium signaling, and IL-17 signaling. (**B**): Bar graph summarizing the same top 20 pathways, ranked by −log10 (P-value).

https://doi.org/10.2147/DDDT.S518696

cell necrosis in the right sensorimotor cortex region, which appeared white (Figure 6A). The other red areas were normal brain tissue with active cells. MRI T2-weighted images showed significant high signal in the right sensorimotor cortex, suggesting acute infarction (Figure 6B). This indicates that the photothrombotic focal stroke model has good consistency and reproducibility. On day 30 after cerebral ischemia, MRI T2-weighted images showed tissue necrosis and liquefaction at the infarct site, forming a cystic cavity (Figure 6B). There were no significant variations in infarct size among the stroke, ZGP-treated, and cysteamine-treated groups (p =0.536, Figure 6B and C).

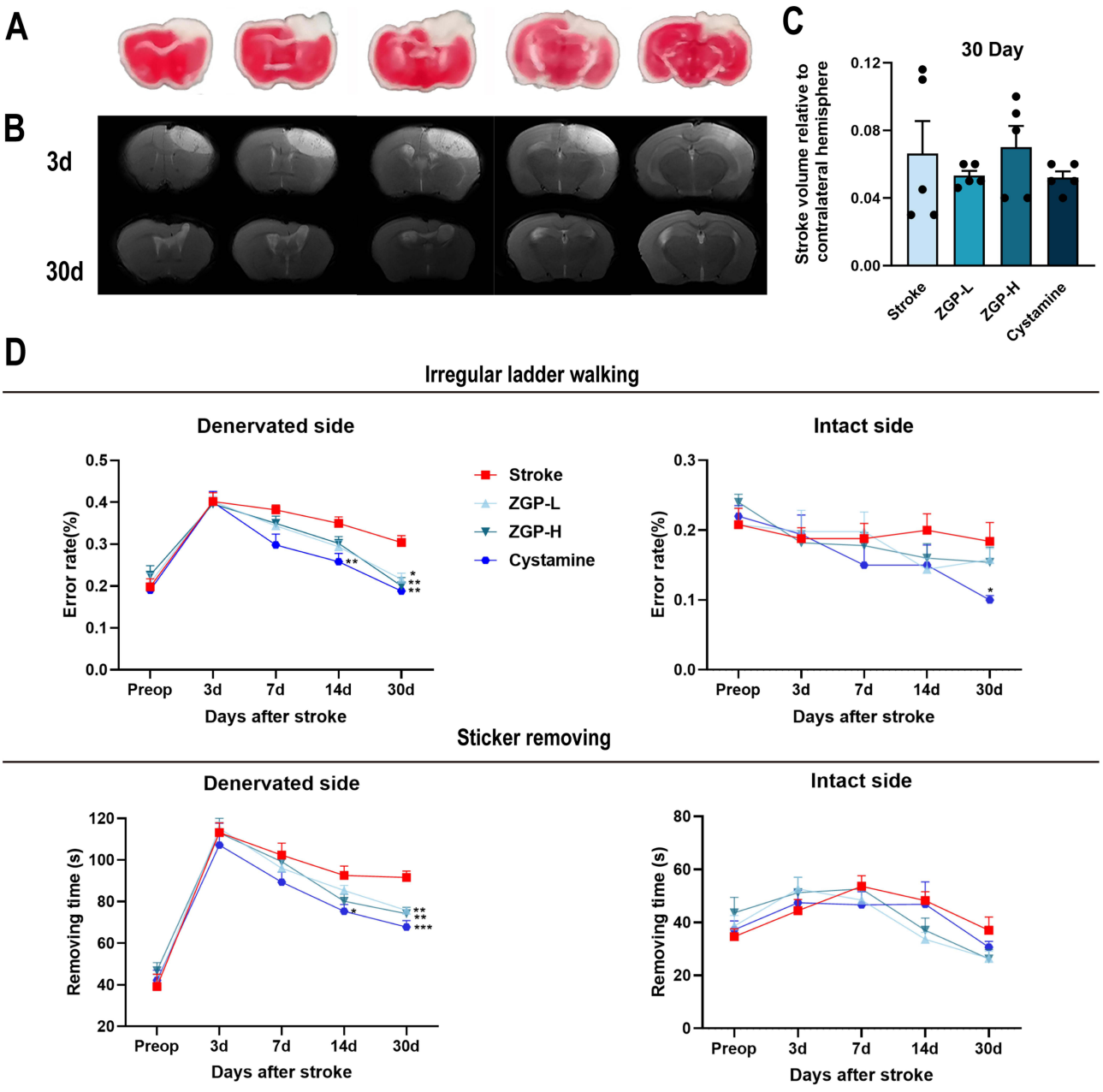

Figure 6 Photothrombotic (PT) stroke model and the impact of ZGP on functional recovery following stroke. **(A)**: Representative distinct pale infarct area was observed in TTC staining 3 days after focal stroke induced by photothrombotic method. (**B**): Representative focal infarcts in the right sensorimotor cortex were demonstrated by T2-weighted images at 3 days and 30 days after photothrombotic focal stroke. **(C)**: Measurement of infarct volume at 30 days. **(D)** Functional recovery was evaluated through irregular ladder walking and sticker removing experiments. Data are expressed as the mean ± SEM (n=5). * p<0.05, ** p<0.01, *** p<0.001, relative to the stroke cohort.

ZGP Promotes Functional Recovery in Mice Following Ischemic Stroke

To evaluate ZGP's therapeutic effects on post-stroke functional recovery, motor and sensory functions were assessed using irregular ladder walking and sticker removing tests. In the irregular ladder walking test, the error rate of the injured forelimb increased to approximately 50% across all groups by day 3 post-stroke, significantly higher than pre-stroke baselines. From days 14 to 30, the cysteamine group (positive control) showed a markedly lower error rate compared to the stroke group ($p = 0.006$, Figure 6D). By day 30, both ZGP-L (3.7 g/kg) and ZGP-H (7.4 g/kg) groups achieved error rates comparable to the cysteamine group ($p = 0.682$ and $p = 0.962$, respectively), with both doses demonstrating significant improvement over the stroke group ($p = 0.013$ and $p = 0.003$, respectively, Figure 6D). In the uninjured forelimb, no significant differences were observed among groups ($p > 0.05$, Figure 6D), except that the cysteamine group exhibited a significantly lower error rate compared to the stroke group ($p = 0.031$, Figure 6D). Similar to the results of irregular ladder walking, the sticker removal test revealed that ZGP-L, ZGP-H, and cysteamine groups exhibited significantly shorter removal times for the injured forelimb compared to the stroke group at day 30 ($p = 0.006$, $p = 0.003$, and $p < 0.001$, respectively, Figure 6D). There was no significant difference in the removal times of the uninjured forelimb among the groups ($p>0.05$, Figure 6D). These data collectively demonstrate that ZGP enhances sensorimotor recovery in ischemic stroke mice, with efficacy comparable to the positive control cysteamine.

Effects of ZGP on Brain Tissue Surrounding Infarct Lesion

Nissl staining revealed distinct histopathological differences between the contralateral normal cortex and peri-infarct regions. In the contralateral normal cortex, neurons were densely packed, uniformly stained, and exhibited well-organized laminar architecture with clearly defined cellular boundaries (Figure 7A). In contrast, the peri-infarct tissue of stroke mice displayed marked structural degradation, including neuronal loss, cytoplasmic-nuclear boundary blurring, vacuolation, connective tissue hyperplasia at lesion margins, and fragmented or faintly stained Nissl bodies. Compared to the stroke group, mice treated with ZGP-L, ZGP-H, and cysteamine showed attenuated tissue damage, characterized by reduced neuronal loss, fewer vacuoles, preserved cellular morphology with sharp cytoplasmic boundaries, and abundant Nissl substance (Figure 7A). These findings suggest that ZGP mitigates post-stroke histopathological degeneration in peri-infarct regions.

ZGP Promotes Angiogenesis and Vascularization in the Sensory Motor Cortex After Stroke

To determine the potential role of ZGP in vascular regeneration, Glut-1 and BrdU-labeled vessels were detected by immunofluorescence staining to assess angiogenesis and vascularization 14 days after cerebral ischemia. As seen in Figure 7B, the peri-infarct regions of ZGP-L, ZGP-H, and cysteamine-treated mice exhibited significantly higher counts of BrdU-positive cells (ZGP-L vs Stroke: $p = 0.049$; ZGP-H vs Stroke: $p = 0.030$; Cysteamine vs Stroke: $p < 0.001$), Glut-1/BrdU double-labeled vessels (ZGP-L vs Stroke: $p = 0.003$; ZGP-H vs Stroke: $p = 0.018$; Cysteamine vs Stroke: $p = 0.001$), and Glut-1-positive vessels (ZGP-L vs Stroke: $p = 0.007$; ZGP-H vs Stroke: $p = 0.048$; Cysteamine vs Stroke: $p = 0.044$) compared to the stroke group (Figure 7B–E). No significant differences were observed among the ZGP-L, ZGP-H, and cysteamine groups in BrdU-positive cells, Glut-1/BrdU double-labeled vessels, or Glut-1 labeled vessels ($p > 0.05$, Figure 7B–E). These results demonstrate that ZGP successfully enhanced angiogenesis and increased Glut-1-positive vessel density in post-stroke brain tissue, suggesting its potent pro-angiogenic effects.

ZGP Promotes Neurogenesis and Neuroblast Migration in Mice After Ischemic Stroke

Following focal ischemia, neuroblasts originating from the subventricular zone (SVZ) of the lateral ventricles proliferate and migrate toward the ischemic lesion. These migrating neuroblasts can be identified by their expression of doublecortin (DCX). To evaluate ZGP's effects on neuroblast proliferation and migration, immunofluorescence double staining for BrdU (proliferation marker) and DCX was performed at 14 days post-stroke. As shown in Figure 8A, a substantial number of BrdU- and DCX-positive cells were observed in the SVZ of stroke mice. Compared to the stroke-only group, both ZGP-L and ZGP-H treatments significantly increased the number of BrdU-positive cells (ZGP-L vs Stroke: $p = 0.009$; ZGP-H vs Stroke: $p = 0.032$), DCX-positive cells (ZGP-L vs Stroke: $p = 0.023$; ZGP-H vs Stroke: $p = 0.035$), and

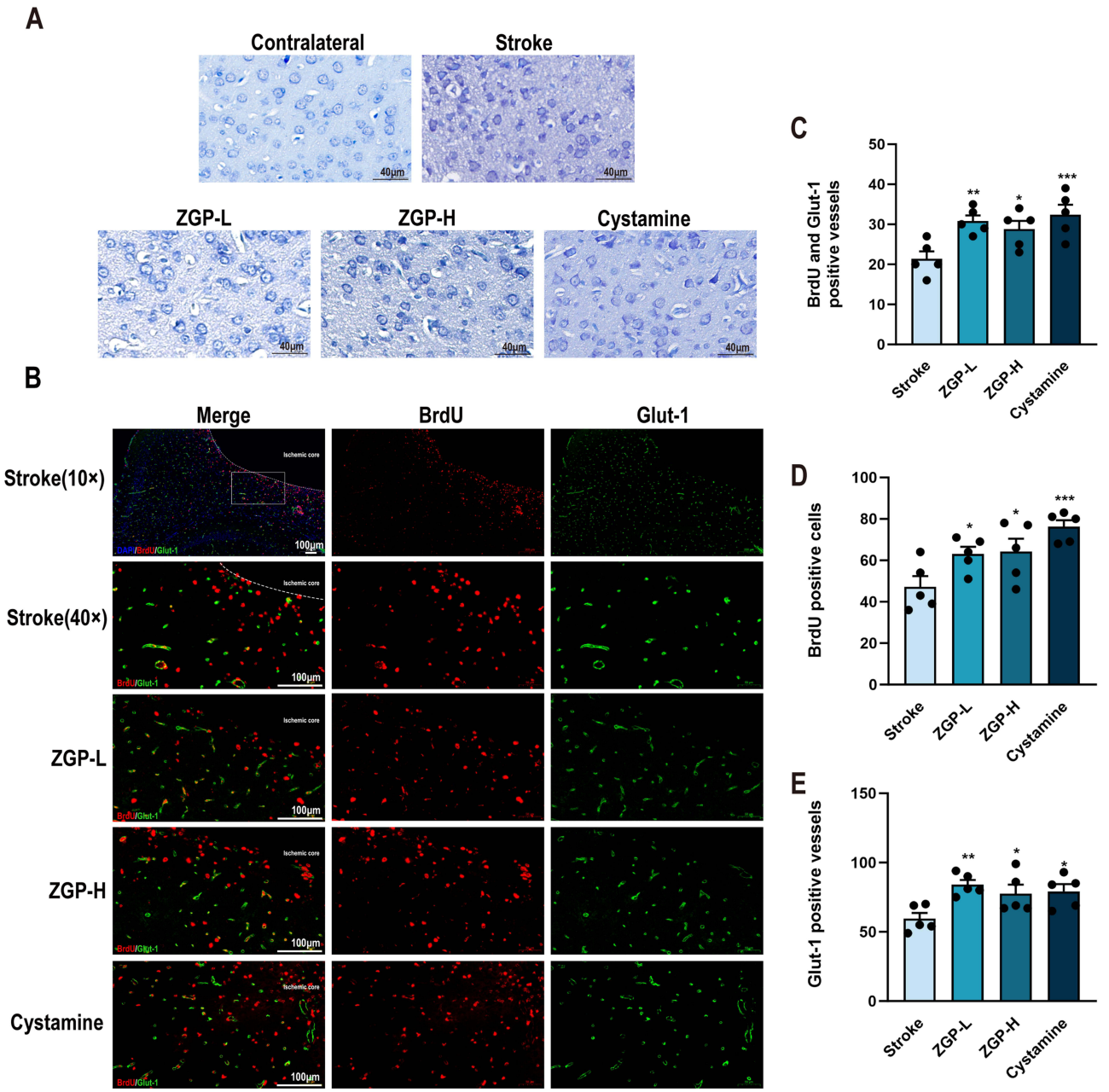

Figure 7 Effects of ZGP on histopathology and angiogenesis in the sensory motor cortex at 14 days after stroke. (**A**): Typical pictures of Nissl staining in the area surrounding the infarct of the sensory motor cortex of mice in different groups. (**B**): Immunostaining for the endothelial cell marker Glut-1 and the proliferation marker BrdU was used to identify angiogenesis and vessel density in the area surrounding the infarct. Dual-positive staining for Glut-1 (green) and BrdU (red), along with the combined Glut-1/BrdU image from mice across various groups. (**C**): Quantification of vessels double-positive for Glut-1/BrdU was demonstrated. (**D**): Quantification of cells positive for BrdU was demonstrated. (**E**) The measurement of vessels positive for Glut-1 was demonstrated. Data are expressed as the mean ± SEM (n=5). * p<0.05, ** p<0.01, *** p<0.001, in comparison to the stroke cohort. Scale bars in (**A**) = 40 μm; Scale bars in (**B**) =100μm.

BrdU/DCX double-positive cells (ZGP-L vs Stroke: p = 0.017; ZGP-H vs Stroke: p = 0.014) (Figure 8A–D). No significant differences were observed between ZGP-treated groups and the cysteamine positive control (p > 0.05, Figure 8A–D). Furthermore, neuroblast migration was assessed in the white matter tract between the infarcted cortex and ipsilateral SVZ (Figure 8E and F). ZGP-L, ZGP-H, and cysteamine treatments significantly elevated DCX-positive cell density in this region (ZGP-L vs Stroke: p = 0.015; ZGP-H vs Stroke: p = 0.021; Cysteamine vs Stroke: p = 0.009) (Figure 8F and G). Notably, DCX-positive cells in ZGP-treated mice migrated farther from the SVZ compared to the stroke-only group. These results indicate that ZGP enhances both the proliferation of neural progenitor cells in the SVZ and their directed migration toward the ischemic lesion.

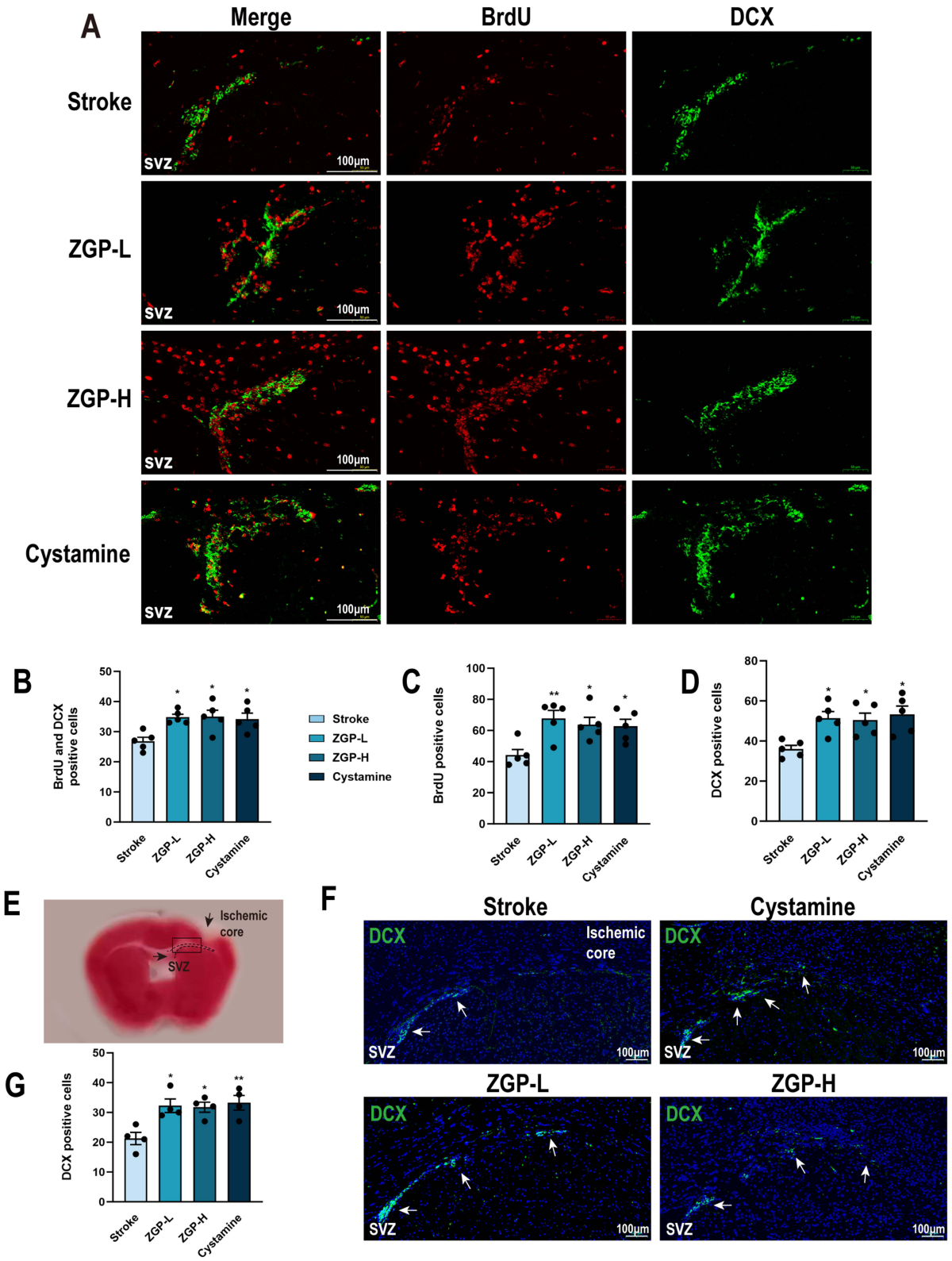

Figure 8 Effects of ZGP on neurogenesis and neuroblast migration at 14 days after stroke. **(A)**: Typical dual immunofluorescent staining pictures of BrdU (red), DCX (green) and merged pictures in the same side of SVZ in different groups. **(B)**: The count of BrdU/DCX double-labeled cells in the SVZ was displayed. (**C**): The number of BrdU positive cells in SVZ was shown. (**D**): The quantity of DCX-positive cells in the SVZ was displayed. (**E**): The study focused on the migration of neuronal cells within the white matter (boxed area) located between the damaged lesion (white) and the same side SVZ. **(F)**: Typical immunofluorescent staining pictures of DCX (green) in the white matter between the ischemic cortex and ipsilateral SVZ. (**G**): Quantification of DCX labeled cells was shown between the ischemic cortex and ipsilateral SVZ. Data are expressed as the mean ± SEM (n=5). * p<0.05, ** p<0.01, compared to the stroke group. Scale bars = 100 μm.

https://doi.org/10.2147/DDDT.S518696

ZGP Promotes Corticospinal Tract Axon Remodeling After Stroke

The aforementioned results demonstrated that ZGP enhanced neurological recovery, angiogenesis, and neurogenesis in cerebral ischemia mice. To further evaluate its long-term effects on axonal remodeling, in vivo DTI was performed 30 days post-stroke, with fractional anisotropy (FA)—a key DTI parameter reflecting white matter integrity—analyzed across five corticospinal tract (CST) regions: Genu, Body, Dorsal fornix, Dorsal syndesis, and Dentate gyrus (Figure 9A). On the ipsilateral side of injury, ZGP-L, ZGP-H and cysteamine treatments significantly increased FA values in at least four CST regions compared to the stroke group ($0.001<p<0.05$), with no significant differences between ZGP and cysteamine groups ($p > 0.05$) (Figure 9B). Contralaterally, FA values showed no group differences except in the Genu, where cysteamine exhibited higher values than the stroke group ($p = 0.015$) (Figure 9C). Fiber tracking further revealed that ZGP and cysteamine significantly increased ipsilateral fiber density at the Genu (sensorimotor cortex) and Dentate gyrus (internal capsule) compared to the stroke group ($0.001<p<0.01$, Figure 10A and B). No differences were observed among treated groups ($p > 0.05$), while contralateral fiber density showed a non-significant upward trend ($p > 0.05$, Figure 10A–C). Collectively, these findings indicate that ZGP promotes CST axon remodeling, particularly in ipsilateral regions, aligning with its functional recovery benefits observed in behavioral and histological assays.

ZGP Enhances the Expression of VEGF, BDNF and p-mTOR Proteins

To elucidate the mechanisms underlying ZGP's therapeutic effects, Western blot analysis was performed on peri-infarct tissues 30 days post-stroke to quantify levels of mTOR, p-mTOR, and neurovascular regeneration markers VEGF and BDNF (Figure 11A). Compared to the stroke group, the ZGP-H and cysteamine groups exhibited significantly elevated VEGF (ZGP-H vs Stroke: $p = 0.002$; Cysteamine vs Stroke: $p = 0.010$), BDNF (ZGP-H vs Stroke: $p = 0.002$; Cysteamine vs Stroke: $p = 0.050$), and p-mTOR/mTOR ratios (ZGP-H vs Stroke: $p < 0.001$; Cysteamine vs Stroke: $p = 0.031$) (Figure 11A–D). Compared to the stroke group, the ZGP-L group exhibited elevated VEGF($p=0.723$), BDNF($p=0.306$), and p-mTOR/mTOR ratio levels, with the p-mTOR/mTOR ratio showing a statistically significant difference ($p=0.008$, Figure 11B–D). Full original Western blot images corresponding to all experimental groups are provided in Figure S1. The above findings indicate that the promotion of neurovascular regeneration and axonal remodeling by ZGP may be associated with the upregulation of VEGF and BDNF expression and activation of mTOR signaling pathway.

Discussion

While ischemic stroke induces massive cell death within the ischemic lesion, it also induces neurovascular regeneration responses in peri-infarct and more distant regions of the ischemic lesion.[20] These responses involve two interconnected processes: angiogenesis and neuroregeneration, the latter comprising neurogenesis and axonal remodeling.[21] However, the regenerative and reparative capacity of adult neural tissue is severely limited, and the extent of spontaneous regenerative repair induced by cerebral ischemia falls far short of clinical rehabilitation demands.[22] Consequently, exploring pharmacological agents and therapeutic approaches to promote neurovascular regeneration and repair represents a pivotal strategy for enhancing functional recovery in ischemic stroke.

Recent advances in neurovascular regeneration highlight the potential of multi-target strategies to address post-stroke recovery. Cutting-edge approaches, such as exosome-mediated BDNF delivery[23] and immune-neurovascular crosstalk regulated by immunomodulatory hydrogel microspheres,[24] enhance angiogenesis and axonal remodeling but face challenges in specificity and clinical translation. In contrast, TCM compound preparations, characterized by multi-component synergy, multi-pathway modulation, and low toxicity, offer unique advantages for ischemic stroke treatment.[25,26] For instance, Naotaifang alleviates ischemic stroke-induced brain injury by modulating microglial polarization to suppress neuroinflammation and ferroptosis,[27,28] while also mitigating neuronal damage through restoring mitochondrial fission/fusion homeostasis.[29] Despite these advances, research on the therapeutic effects of TCM in promoting neurovascular regeneration and repair after cerebral ischemia remains limited, underscoring the need for further mechanistic exploration. As a representative TCM formula, Zuogui Pill (ZGP) has been used since the Ming Dynasty to nourish kidney yin and replenish marrow. Our prior studies identified 76 bioactive compounds in ZGP via UPLC-QTOF-MS, including 14 high-abundance components.[16] These active ingredients have various biological effects, for example, anti-oxidant and anti-

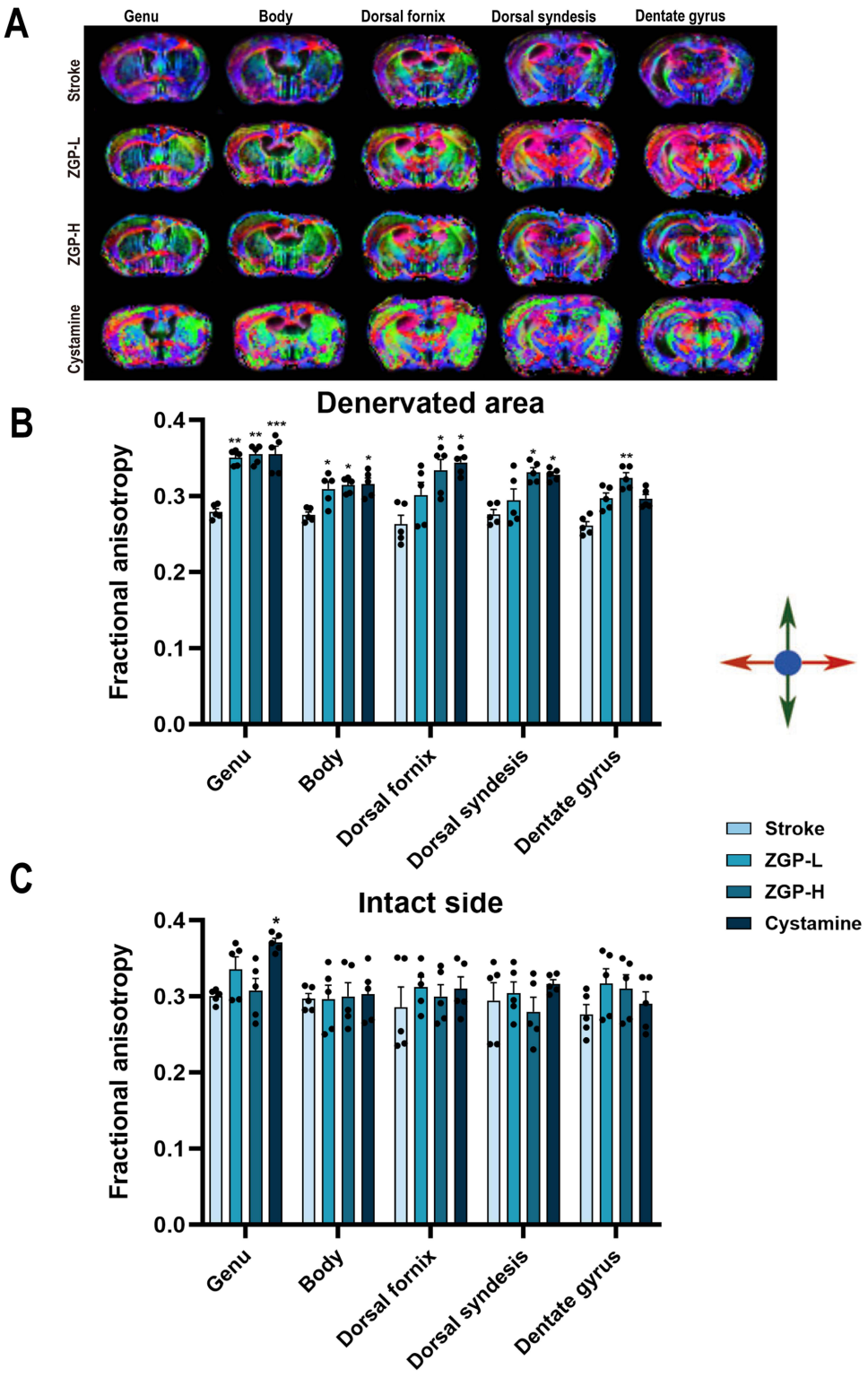

Figure 9 Effect of ZGP on corticospinal tract axon remodeling. **(A)**: FA color maps of representative orientation coding of typical brains from different groups of mice in five different levels from the dentate gyrus of hippocampus to the genu. Orientation of fiber trajectories is color-coded, with green showing the anterior and posterior directions, blue demonstrating the superior and inferior directions, and red indicating the left and right directions. (**B**): FA values measured in the levels of Genu, Body, Dorsal fornix, Dorsal syndesis, and Dentate gyrus in the ipsilateral side of the injury from different groups of mice. (**C**): FA values quantified in the contralateral side of the injury at the same locations as in (B). Data are expressed as the mean ± SEM (n=5). * p<0.05, ** p<0.01, *** p<0.001, in contrast to the stroke cohort.

https://doi.org/10.2147/DDDT.S518696

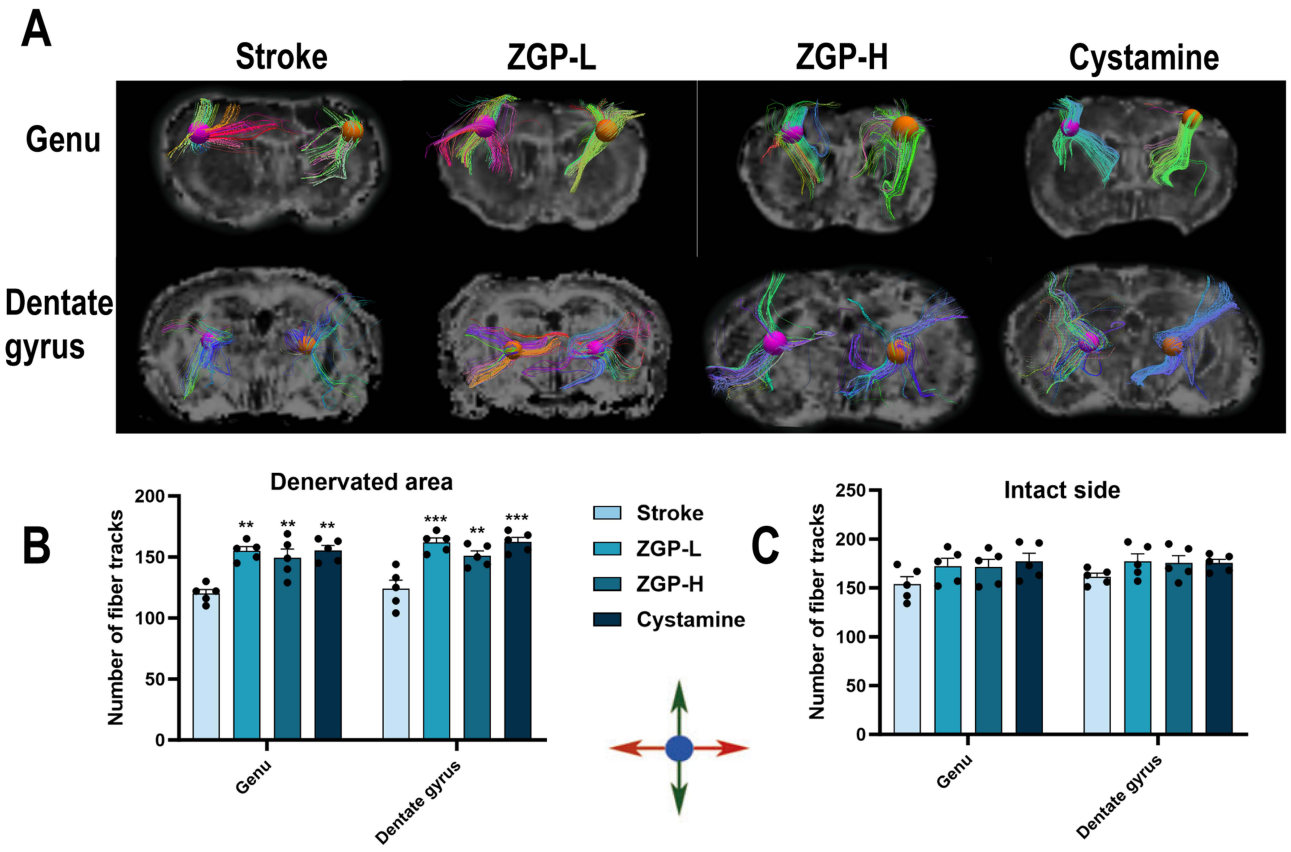

Figure 10 The role of ZGP in the sensorimotor fiber tracking. **(A)**: Typical photos of multi-dimensional fiber tracing of ROI at the levels of genu and dentate gyrus in different groups of mice 30 days after stroke. The ROI radius is 0.468 mm. Color coding is employed to show the fiber tracing direction: green for anterior and posterior, red for left and right, and blue for superior and inferior. (**B**): Quantitative assessment of fiber tracking density within the regions of interest at the genu and dentate gyrus levels in various groups of mice in the ipsilateral side of the injury. (**C**): Quantitative analysis of fiber tracking intensity of ROI at levels of genu and dentate gyrus in different groups of mice in the contralateral side of the injury. Data are expressed as the mean ± SEM (n=5). ** p<0.01, *** p<0.001, compared to the stroke cohort.

inflammatory, immune enhancement, neuroprotection, promotion of axonal regeneration and neurite's outgrowth, and improvement of cognition and memory.[16] Our clinical trials confirm ZGP's efficacy in improving neurological outcomes in stroke patients.[11] The basic researches have shown that ZGP can enhance axonal regeneration and crossing ability of neural cells in vitro, promote axonal growth and restore neural function in ischemic stroke mice.[13,16,17] Moreover, research by Liu et al[30] indicates that ZGP can suppress inflammation, safeguard neurons, and improve cognitive function. However, whether ZGP promotes angiogenesis and neurogenesis post-stroke has not been systematically investigated until this study.

In this study, we employed network pharmacology to elucidate the mechanisms underlying ZGP's therapeutic effects on ischemic stroke, with a focus on neurovascular regeneration. Through systematic screening, we identified quercetin, beta-sitosterol, isorhamnetin, hydroxygenkwanin, and kaempferol as ZGP's core components promoting post-stroke neurovascular repair. These compounds have been extensively documented to enhance synaptic plasticity, stimulate vascular endothelial cell proliferation/differentiation, and improve cognitive function.[31–33] Mechanistically, they activate the Cyclic AMP Response Element-Binding Protein (CREB) /BDNF signaling pathway and modulate Mitogen-Activated Protein Kinase (MAPK), mTOR, and VEGF cascades.[33,34] PPI network analysis prioritized 20 high-confidence targets for ZGP, with mTOR emerging as a central node. mTOR is a crucial signaling molecule that regulates the inherent capacity of neurovascular cells to develop. Our team's previous research has found that the mTOR pathway is inhibited in the adult nervous system.[35] By reactivating the mTOR pathway, it was able to promote the regeneration of optic nerve axons and recovery of vision after optic nerve injury, and significant regeneration of CST axons as well as recovery of neurological function after spinal cord injury and cerebral ischemia.[14,36] Therefore, activating the mTOR pathway can stimulate intrinsic growth ability and promote the regeneration and repair of brain tissue. In addition, there is evidence to

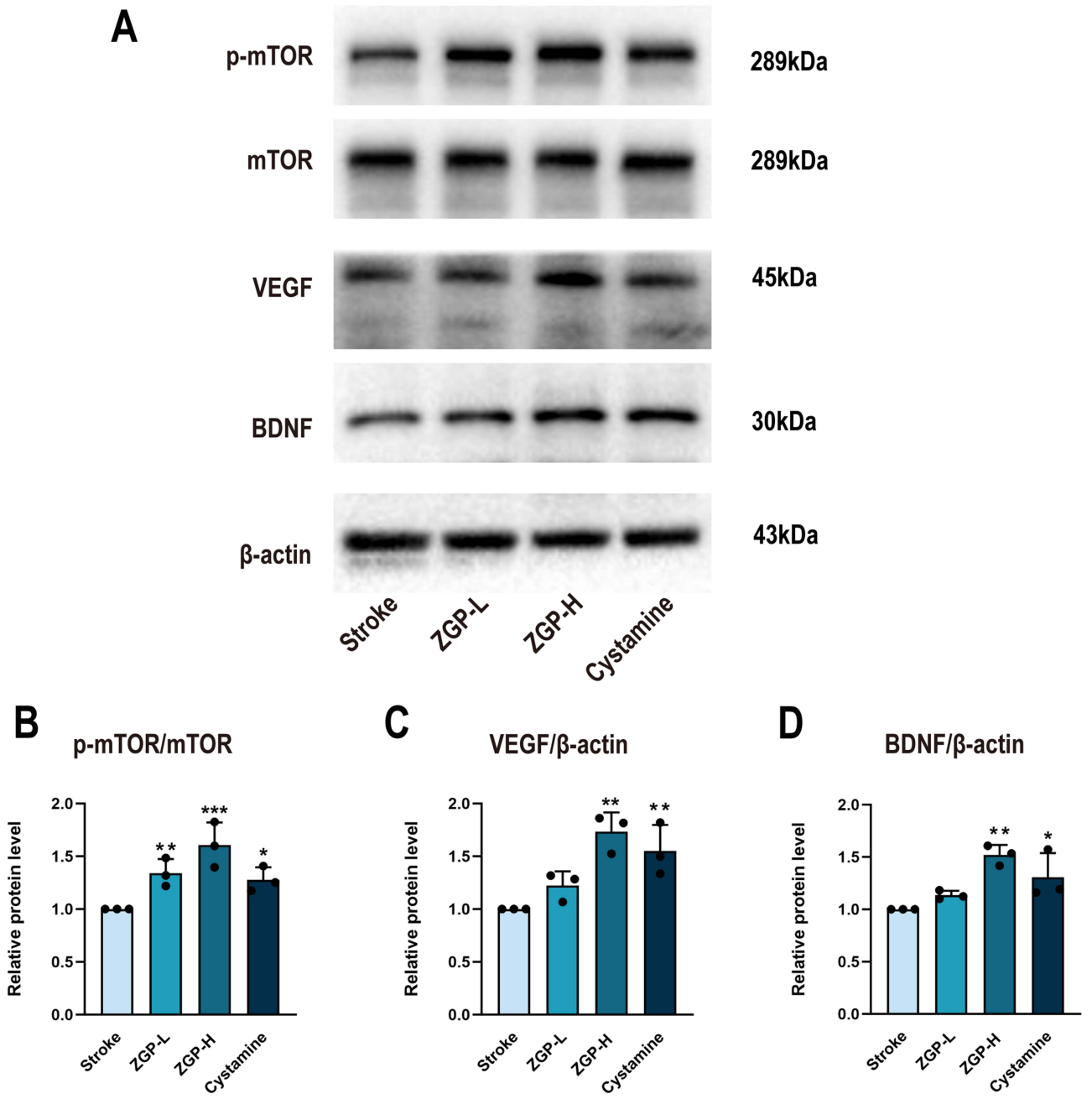

Figure 11 Impact of ZGP on BDNF, VEGF, mTOR, and p-mTOR proteins expression. **(A)**: Typical photographs of Western blot for BDNF, VEGF, mTOR, and p-mTOR in ischemic brain 30 days post-stroke in various groups. **(B)**: The p-mTOR/mTOR ratio in ischemic brain tissues was quantified by normalization to β-actin. (**C**): Quantitative expression of VEGF in tissues around the infarct lesion. (**D**) Quantitative expression of BDNF in tissues around the infarct lesion. Data are expressed as the mean ± SEM (n=3). * p<0.05, ** p<0.01, *** p<0.001, compared to the stroke cohort.

suggest that BDNF can promote neuronal differentiation and facilitate axonal growth through activating the mTOR signaling pathway.[37] Furthermore, VEGF/VEGF receptor 2 interaction triggers mTOR signaling to drive endothelial proliferation and vascular lumen formation,[9,38] synergistically enhancing ZGP's neurovascular regenerative capacity.

Employing a photothrombotic focal cerebral ischemia rodent model, we demonstrated that ZGP promotes angiogenesis, neurogenesis, and function recovery post-stroke. To evaluate its therapeutic effects during the subacute recovery phase, ZGP treatment was initiated on day 3 post-ischemia. Angiogenesis and neurogenesis were assessed via Glut-1/ BrdU and DCX/ BrdU dual labeling, respectively. After 14 days of ZGP administration, peri-infarct regions exhibited a

https://doi.org/10.2147/DDDT.S518696

marked increase in Glut-1+/ BrdU+ endothelial cells and vascular density, confirming ZGP's pro-angiogenic effects (Figure 7B-E). Concurrently, ZGP enhanced neural progenitor cell proliferation in the subventricular zone (SVZ), evidenced by elevated DCX+/BrdU+ cell counts, and facilitated their migration toward ischemic lesions (Figure 8A-G). By day 30, ZGP-treated mice showed significant sensorimotor functional recovery, with error rates in ladder walking reduced and sticker removal time shortened compared to stroke controls (Figure 6D). These findings provide direct experimental evidence that ZGP concurrently enhances vascular and neural regeneration, offering a promising therapeutic strategy for ischemic stroke recovery.

We further elucidated the mechanisms by which ZGP promotes neurovascular regeneration and functional recovery. Post-stroke repair involves dual strategies: optimizing the regenerative microenvironment and enhancing intrinsic cellular repair capacity.[22] It is widely recognized that boosting VEGF and BDNF levels can enhance the regenerative environment following cerebral ischemia, aiding in neurovascular growth and axonal restructuring. Furthermore, VEGF induction triggers BDNF secretion from endothelial cells, creating a feedforward loop that enhances neuronal survival and circuit reorganization.[23] Western blot analysis of peri-infarct tissues at 30 days post-stroke revealed that ZGP significantly increased VEGF and BDNF levels while elevating the p-mTOR/mTOR ratio compared to stroke controls (Figure 11A-D). These results indicate that ZGP orchestrates brain repair through coordinated actions: enhancing regenerative factor secretion (BDNF/VEGF) to improve microenvironmental support, while reactivating mTOR signaling to potentiate intrinsic neurovascular growth pathways. This dual mechanism maximizes endogenous repair potential, as illustrated in our integrated model (Figure 12).

Axonal remodeling is a critical component of post-stroke brain repair. The corticospinal tract (CST)—a major projection fiber bundle connecting the sensorimotor cortex and spinal cord—plays a pivotal role in sensorimotor function

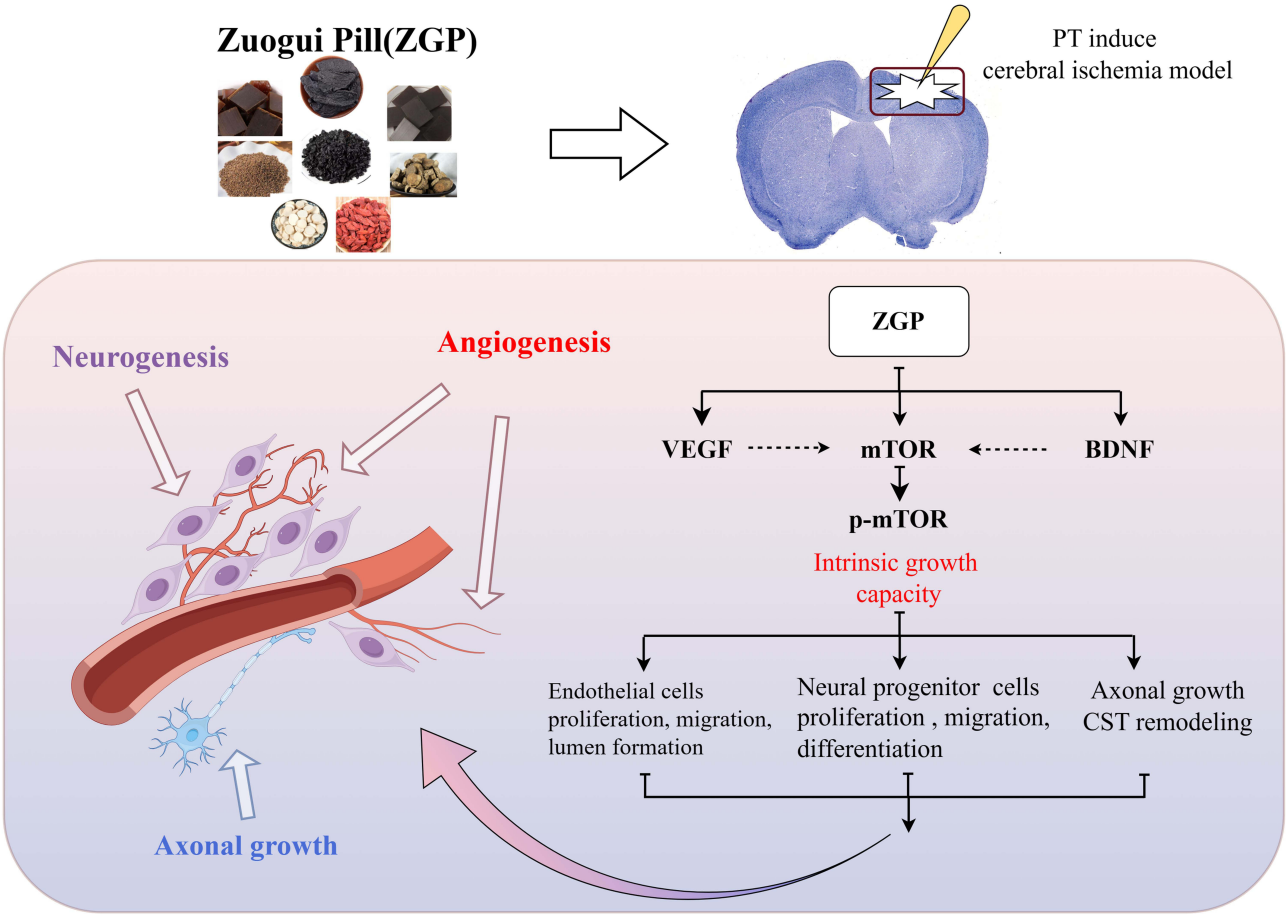

Figure 12 ZGP's mechanisms of action for accelerating ischemic stroke recovery.

recovery through axon regeneration, collateral sprouting, and neural network reorganization following cerebral ischemia. Diffusion tensor imaging (DTI), a noninvasive MRI technique leveraging water molecule' anisotropic diffusion, provides precise quantification of white matter microstructure.[39] DTI-derived fractional anisotropy (FA) values enable three-dimensional CST reconstruction, revealing axonal integrity, myelination status, and fiber density. Reduced FA correlates with CST axonal loss and functional deficits, making it a validated biomarker for monitoring treatment-induced recovery.[40] In this study, DTI analysis at 30 days post-stroke demonstrated that ZGP treatment significantly increased ipsilateral CST axon density and integrity, as confirmed by a marked elevation in FA values, comparable to the positive control cysteamine (Figure 9A-B). Fiber tracking revealed that ZGP restored orderly sensorimotor axon projections to the internal capsule, counteracting stroke-induced fiber loss and disorganization (Figure 10A-B). Crucially, ZGP's lack of effect on infarct volume underscores that its therapeutic efficacy arises from enhancing peri-infarct plasticity rather than reducing acute ischemic damage, aligning with the core principles of subacute therapeutic strategies.

While this study elucidates ZGP's role in promoting neurovascular regeneration and corticospinal tract remodeling, certain limitations should be acknowledged. First, the impact of ZGP on blood-brain barrier (BBB) repair—a critical mediator of neurovascular coupling and post-stroke recovery —was not directly assessed. Future studies employing BBB-specific markers and functional permeability assays will address these gaps. Second, while we identified mTOR signaling as a central mechanism, ZGP's interactions with related pathways—particularly insulin-like growth factor-1 (IGF-1)/ osteopontin (OPN)/ phosphatase and tensin homolog deleted on chromosome ten (PTEN) crosstalk—and its effects on axonal remodeling markers (growth-associated protein 43 [GAP43], myelin basic protein [MBP], synapsin1 [SYN1]) remain incompletely characterized. Systematic interrogation using pathway-specific inhibitors (eg, linsitinib for IGF-1 receptor, rapamycin for mTOR) and spatial transcriptomics will clarify these mechanisms. These limitations highlight the need for further mechanistic exploration to optimize ZGP's therapeutic potential in ischemic stroke.

Conclusion

Our research results indicate that ZGP can induce neurogenesis and angiogenesis, enhance CST remodeling, and facilitate the recovery of mice's neurological function following a focal stroke. The mechanisms by which ZGP produces these impacts are connected with the regulation of VEGF and BDNF expression, and activating the mTOR pathway. These findings provide the first direct evidence that ZGP—a kidney-nourishing TCM formula—bridges neurovascular repair by simultaneously upregulating trophic factors (VEGF, BDNF) and reactivating mTOR-dependent regenerative pathways. Future studies should explore ZGP's impact on blood-brain barrier restoration and validate signaling pathways' crosstalk using pathway-specific inhibitors. Clinical translation via multimodal neuroimaging (eg, DTI-coupled perfusion MRI) will further elucidate its therapeutic potential in stroke patients.

Abbreviations

ZGP, Zuogui Pill; IS, Ischemic stroke; CST, corticospinal tract; TTC, 2,3,5-triphenyl-2H-tetrazolium chloride; DTI, diffusion tensor imaging; BDNF, brain-derived neurotrophic factor; VEGF, vascular endothelial growth factor; mTOR, mammalian target of rapamycin; p-mTOR, phosphor-mammalian target of rapamycin; BrdU, 5-bromo-20-deoxyuridine; DCX, doublecortin; SVZ, subventricular zone; Glut-1, glucose transporter type 1; FA, fractional anisotropy; WHO, World Health Organization; ROIs, Regions of interests; ANOVA, One-way analysis of variance.

Ethics Statement

The animal study protocol in the study was approved by the Animal Ethics Committee of Affiliated Hospital of Nanjing University of Chinese Medicine (2021 DW-04-02, February 9, 2021).

Author Contributions

All authors made a significant contribution to the work reported, whether that is in the conception, study design, execution, acquisition of data, analysis and interpretation, or in all these areas; took part in drafting, revising or critically reviewing the article; gave final approval of the version to be published; have agreed on the journal to which the article has been submitted; and agree to be accountable for all aspects of the work.

Funding

This work was supported by National Natural Science Foundation of China (Grant No. 82474435,81973794), Natural Science Foundation of Jiangsu Province (Grant No. BK20241996), Academic Degree and Postgraduate Education Reform Project of Jiangsu Province (Grant No. SJCX24_1012).

Disclosure

The authors report no conflicts of interest in this work.

References

1. Saini V, Guada L, Yavagal DR. Global epidemiology of stroke and access to acute ischemic stroke interventions. *Neurology*. 2021;97(20 Suppl 2):S6–S16. doi:10.1212/WNL.0000000000012781
2. Emberson J, Lees KR, Lyden P, et al. Effect of treatment delay, age, and stroke severity on the effects of intravenous thrombolysis with alteplase for acute ischaemic stroke: a meta-analysis of individual patient data from randomised trials. *Lancet*. 2014;384(9958):1929–1935. doi:10.1016/S0140-6736(14)60584-5
3. Rust R, Grönnert L, Gantner C, et al. Nogo-A targeted therapy promotes vascular repair and functional recovery following stroke. *Proc Natl Acad Sci USA*. 2019;116(28):14270–14279. doi:10.1073/pnas.1905309116
4. Nagase T, Kin K, Yasuhara T. Targeting neurogenesis in seeking novel treatments for ischemic stroke. *Biomedicines*. 2023;11(10):2773. doi:10.3390/biomedicines11102773
5. Mirzahosseini G, Adam JM, Nasoohi S, et al. Lost in translation: neurotrophins biology and function in the neurovascular unit. *Neuroscientist*. 2023;29(6):694–714. doi:10.1177/10738584221104982
6. Yanev P, van Tilborg GA, van der Toorn A, et al. Prolonged release of VEGF and Ang1 from intralesionally implanted hydrogel promotes perilesional vascularization and functional recovery after experimental ischemic stroke. *J Cereb Blood Flow Metab*. 2022;42(6):1033–1048. doi:10.1177/0271678X211069927
7. Gao J, Yao M, Chang D, et al. mTOR (Mammalian Target of Rapamycin): hitting the bull's eye for enhancing neurogenesis after cerebral ischemia? *Stroke*. 2023;54(1):279–285. doi:10.1161/STROKEAHA.122.040376
8. Li MX, Weng JW, Ho ES, et al. Brain delivering RNA-based therapeutic strategies by targeting mTOR pathway for axon regeneration after central nervous system injury. *Neural Regeneration Research*. 2022;17(10):2157–2165. doi:10.4103/1673-5374.335830
9. Takei N, Nawa H. mTOR signaling and its roles in normal and abnormal brain development. *Front Mol Neurosci*. 2014;7:28. doi:10.3389/fnmol.2014.00028
10. Li J, Zhao X, Zhang Y, et al. Comparison of traditional Chinese medicine in the long-term secondary prevention for patients with ischemic stroke: a systematical analysis. *Front Pharmacol*. 2021;12:722975. doi:10.3389/fphar.2021.722975
11. Li WL, Li L, Wu MH. Effect of zuogui pill on movement disorder in patients with ischemic stroke. *J Changchun Univ Chin Med*. 2019;35(05):872–875. doi:10.13463/j.cnki.cczyy.2019.05.017
12. Liu JF, Shu Q, Zhang Y. Protective effective and mechanism of zuogui pill-containing serum on oxygen and glucose deprivation injury of hippocampal neurons and glial cells in rat. *Shanxi Med J*. 2022;51(01):15–19.
13. Liu Y, Gao CC, Li L, et al. Effect and mechanism of Zuogui Pills on neural function recovery in ischemic stroke mice based on OPN/IGF-1/mTOR. *Zhongguo Zhong Yao Za Zhi*. 2023;48(19):5250–5258. doi:10.19540/j.cnki.cjcmm.20230515.401
14. Liu Y, Wang X, Li W, et al. A Sensitized IGF1 treatment restores corticospinal axon-dependent functions. *Neuron*. 2017;95(4):817–833e4. doi:10.1016/j.neuron.2017.07.037
15. Li PC, Jiao Y, Ding J, et al. Cystamine improves functional recovery via axon remodeling and neuroprotection after stroke in mice. *CNS Neurosci Ther*. 2015;21(3):231–240. doi:10.1111/cns.12343
16. Liu Y, Wu D, Yan X, et al. Zuogui pill promotes neurite outgrowth by regulating OPN/ IGF-1R/PTEN and downstream mtor signaling pathway. *Comb Chem High Throughput Screening*. 2025;28(4):675–690. doi:10.2174/0113862073295309240214060857
17. Li L, Liu Y, Zheng Y, et al. Exploring the mechanisms under Zuogui Pill's treatment of ischemic stroke through network pharmacology and in vitro experimental verification. *Front Pharmacol*. 2023;14:1153478. doi:10.3389/fphar.2023.1153478
18. Li WL, Yu SP, Ogle ME, et al. Enhanced neurogenesis and cell migration following focal ischemia and peripheral stimulation in mice. *Dev Neurobiol*. 2008;68(13):1474–1486. doi:10.1002/dneu.20674
19. Li WL, Fraser JL, Yu SP, et al. The role of VEGF/VEGFR2 signaling in peripheral stimulation-induced cerebral neurovascular regeneration after ischemic stroke in mice. *Exp Brain Res*. 2011;214(4):503–513. doi:10.1007/s00221-011-2849-y
20. Duan H, Li S, Hao P, et al. Activation of endogenous neurogenesis and angiogenesis by basic fibroblast growth factor-chitosan gel in an adult rat model of ischemic stroke. *Neural Regeneration Research*. 2024;19(2):409–415. doi:10.4103/1673-5374.375344
21. Toman NG, Grande AW, Low WC. Neural Repair in Stroke. *Cell Transplant*. 2019;28(9–10):1123–1126. doi:10.1177/0963689719863784
22. He Z, Jin Y. Intrinsic control of axon regeneration. *Neuron*. 90(3):437–451. doi:10.1016/j.neuron.2016.04.022.
23. Zhou X, Deng X, Liu M, et al. Intranasal delivery of BDNF-loaded small extracellular vesicles for cerebral ischemia therapy. *J Control Release*. 2023;357:1–19. doi:10.1016/j.jconrel.2023.03.033
24. Xu T, Gan L, Chen W, et al. Bridging immune-neurovascular crosstalk via the immunomodulatory microspheres for promoting neural repair. *Bioact Mater*. 2025;44:558–571. doi:10.1016/j.bioactmat.2024.10.031
25. Zhou J, Sun F, Zhang W, et al. Novel insight into the therapeutical potential of flavonoids from traditional Chinese medicine against cerebral ischemia/reperfusion injury. *Front Pharmacol*. 2024;15:1352760. doi:10.3389/fphar.2024.1352760
26. Wu B, Zhou D, Mei Z. Targeting the neurovascular unit: therapeutic potential of traditional Chinese medicine for the treatment of stroke. *Heliyon*. 2024;10(19):e38200. doi:10.1016/j.heliyon.2024.e38200
27. Liao J, Wei M, Wang J, et al. Naotaifang formula attenuates OGD/R-induced inflammation and ferroptosis by regulating microglial M1/M2 polarization through BMP6/SMADs signaling pathway. *Biomed Pharmacother*. 2023;167:115465. doi:10.1016/j.biopha.2023.115465

28. Zhou Y, She R, Mei Z, et al. Crosstalk between ferroptosis and necroptosis in cerebral ischemia/reperfusion injury and Naotaifang formula exerts neuroprotective effect via HSP90-GCN2-ATF4 pathway. *Phytomedicine*. 2024;130:155399. doi:10.1016/j.phymed.2024.155399
29. She R, Tian H, Sun F, et al. Naotaifang formula regulates Drp1-induced remodeling of mitochondrial dynamics following cerebral ischemia-reperfusion injury. *Free Radic Biol Med*. 2025;229:139–153. doi:10.1016/j.freeradbiomed.2025.01.031
30. Liu H, Dai Q, Yang J, et al. Zuogui pill attenuates neuroinflammation and improves cognitive function in cerebral ischemia reperfusion-injured rats. *Neuroimmunomodulation*. 2022;29(2):143–150. doi:10.1159/000519010
31. Jadhav R, Kulkarni YA. Neuroprotective Effect of Quercetin and memantine against AlCl(3)-induced neurotoxicity in albino wistar rats. *Molecules*. 2023;28(1). doi:10.3390/molecules28010417
32. Katebi S, Esmaeili A, Ghaedi K, et al. Superparamagnetic iron oxide nanoparticles combined with NGF and quercetin promote neuronal branching morphogenesis of PC12 cells. *Int J Nanomed*. 2019;14:2157–2169. doi:10.2147/IJN.S191878
33. Hu WH, Wang HY, Xia YT, et al. Kaempferol, a major flavonoid in ginkgo folium, potentiates angiogenic functions in cultured endothelial cells by binding to vascular endothelial growth factor. *Front Pharmacol*. 2020;11:526. doi:10.3389/fphar.2020.00526
34. Chen PY, Lin MS, Chen CC, et al. The flavonoid hydroxygenkwanin reduces inflammation and neointimal formation. *J Nutr Biochem*. 2024;135:109771. doi:10.1016/j.jnutbio.2024.109771
35. Park KK, Liu K, Hu Y, et al. Promoting axon regeneration in the adult CNS by modulation of the PTEN/mTOR pathway. *Science*. 2008;322 (5903):963–966. doi:10.1126/science.1161566
36. Bei F, Lee HHC, Liu X, et al. Restoration of visual function by enhancing conduction in regenerated axons. *Cell*. 2016;164(1–2):219–232. doi:10.1016/j.cell.2015.11.036
37. Moya-Alvarado G, Tiburcio-Felix R, Ibanez MR, et al. BDNF/TrkB signaling endosomes in axons coordinate CREB/mTOR activation and protein synthesis in the cell body to induce dendritic growth in cortical neurons. *Elife*. 2023;12:e77455. doi:10.7554/eLife.77455
38. Liu B, Luo C, Zheng Z, et al. Shengui sansheng san extraction is an angiogenic switch via regulations of AKT/mTOR, ERK1/2 and Notch1 signal pathways after ischemic stroke. *Phytomedicine*. 2018;44:20–31. doi:10.1016/j.phymed.2018.04.025
39. Shaheen HA, Sayed SS, Magdy MM, et al. Prediction of motor recovery after ischemic stroke: clinical and diffusion tensor imaging study. *J Clin Neurosci*. 2022;96:68–73. doi:10.1016/j.jocn.2021.12.029
40. Yu X, Jiaerken Y, Wang S, et al. Changes in the corticospinal tract beyond the ischemic lesion following acute hemispheric stroke: a diffusion kurtosis imaging study. *J Magn Reson Imaging*. 2020;52(2):512–519. doi:10.1002/jmri.27066